Computing (2009) 84:149–181
DOI 10.1007/s00607-009-0031-1

A high-order integral algorithm for highly singular PDE solutions in Lipschitz domains

Oscar P. Bruno · Jeffrey S. Ovall · Catalin Turc

Received: 4 November 2008 / Accepted: 6 April 2009 / Published online: 24 April 2009

Abstract We present a new algorithm, based on integral equation formulations, for the solution of constant-coefficient elliptic partial differential equations (PDE) in closed two-dimensional domains with non-smooth boundaries; we focus on cases in which the integral-equation solutions as well as physically meaningful quantities (such as, stresses, electric/magnetic fields, etc.) tend to infinity at singular boundary points (corners). While, for simplicity, we restrict our discussion to integral equations associated with the Neumann problem for the Laplace equation, the proposed methodology applies to integral equations arising from other types of PDEs, including the Helmholtz, Maxwell, and linear elasticity equations. Our numerical results demonstrate excellent convergence as discretizations are refined, even around singular points at which solutions tend to infinity. We demonstrate the efficacy of this algorithm through applications to solution of Neumann problems for the Laplace operator over a variety of domains—including domains containing extremely sharp concave and convex corners, with angles as small as $\pi/100$ and as large as $199\pi/100$.

Keywords Boundary value problems · Second-kind integral equations · Singular solution · High-order methods

Mathematics Subject Classification (2000) 31A05 · 35C15 · 65N35 · 65R20

O. P. Bruno · J. S. Ovall (✉)
California Institute of Technology, Pasadena, CA 91125, USA
e-mail: jovall@acm.caltech.edu

O. P. Bruno
e-mail: bruno@acm.caltech.edu

C. Turc
Case Western Reserve University, Cleveland, OH 44106, USA

1 Introduction

The problem of evaluating numerical solutions of partial differential equations (PDE) under conditions that give rise to solution singularities (such as reduced differentiability and/or blow-up) is one of fundamental importance in science and engineering—yet, a wide variety of such problems have not been adequately addressed from a computational perspective. In this paper, we consider a prototypical problem of this type, namely, solution of the Neumann problem for Laplace's equation in domains containing corners. For this problem, the associated integral-equation solutions, along with the physical fields, tend to infinity at the singular points. The methodology we propose, which is based on use of Nyström discretization of integral equations and exact cancellation of blow-up terms, applies to a variety of other problems for which integral formulations exist, including two- and three-dimensional problems concerning potential theory, scattering and diffraction in areas such as electromagnetics, acoustics and solid mechanics. In this paper, we introduce our algorithm and establish the high-order accuracy of the forward operator; the mathematical analysis of stability and convergence of the method, which are amply demonstrated in this text through a variety of numerical examples, is left for future work. We emphasize that, in particular, the numerical solutions produced by our approach capture the blow-up of physical quantities with a high degree of accuracy.

A variety of high-order integral equation methods for two- and three-dimensional problems in domains with *smooth boundaries* have been available for some time [9,21,35,45]. Both high- and low-order accurate integral equation methods for *non-smooth domains* have been put forward as well [1,10,12,13,18,19,27,28,38]; the references [1,38] are representative of a significant portion of the (sizable) literature on *high order* integral equation approaches. The literature related to reference [1] is discussed in some detail later in this text. The approach represented by the contribution [38], in turn, relies on use of first kind (singular or hypersingular) integral equations and high-order (Galerkin) boundary element methods; such approaches, which apply both to Dirichlet and Neumann problems and are theoretically sound, require costly evaluation of matrix elements and, for cases in which the integral equation solutions are unbounded, have, in practice, given rise to limited accuracies; see e.g. [26].

While not the focus of this paper, for completeness we mention previous contributions concerning finite element methods (FEM) for PDEs on domains with geometric singularities. Although, in contrast with integral equation methods, the FEM give rise to sparse systems of linear equations, these approaches are not competitive with integral-equation methods in some circumstances—since the lower-dimensional integral-equation discretizations can be exploited through use of fast solvers [7,9,43,41], which, when applicable, can outperform their FEM counterparts to very significant extents. FEM based approaches for boundary value problems in domains with singular boundaries are very important in a number of fields, however, and a rich literature has been developed in this area. In [3–5,15–17], for example, spatially refined meshes are used near regions of geometric singularity. An alternative approach, in which the *known* singular behavior is explicitly incorporated into the Galerkin basis, is discussed in [20,29,37,44]. In the "DtN finite element method" approach [25,52,53] neighborhoods of corner singularities are identified, and a new

boundary value problem is posed on the complement of the corner neighborhoods by means of artificial boundary conditions obtained via Dirichlet-to-Neumann maps.

Focusing on previous Nyström methodologies, which are closer in spirit to the approach put forward in the present contribution, on the other hand, we mention [2,22,36]; the extensive literature in this area is discussed in [1, Chap. 8]. Each of these contributions employs special graded-mesh quadratures to achieve high-order accuracy in the solution of the *Dirichlet problem* in two-dimensional domains with corners by means of second-kind integral equations. A direct extension of this methodology to the Neumann case does not generally give rise to highly accurate solutions. A key theoretical and practical difference between the Dirichlet and Neumann problems in this regard, is that the solutions of the corresponding integral equations are bounded for the former (if the integral equations are selected appropriately), while they are unbounded (at corners) for the latter. The contribution [40], which, like [2,22,36], is based on use of changes-of-variables and graded meshes, considers solutions of both Dirichlet and Neumann problems and has produced results of significant accuracy. As demonstrated in Sect. 5, such an approach does not completely resolve the singular corner behavior in the Neumann case, and thus it

1. Cannot yield high accuracies for Neumann problems around corner points, unless expensive, highly refined integration rules are used to evaluate integrals of the products of basis functions and the very highly peaked composition of the nearly non-integrable kernel and the graded-mesh change-of-variables. Even using such expensive integration rules, and for the mild angles considered, the approach [40] yields, for a given discretization size, significantly lower accuracies, by several orders of magnitude, than the present method; and
2. Owing to subtractive cancellations, it leads to diminishing accuracies as discretizations are refined beyond a certain level—yielding limited or no accuracy for problems which, like the sharp-angle problems mentioned below in this text, require fine sampling meshes.

Relying on analytical cancellation of singularities and special treatment of nearly non-integrable integrands (see Remark 3.1 and Sect. 5), the approach we present in this contribution eliminates these difficulties and enables highly efficient high-order Nyström solution of the general *Neumann problems*. In this method, the leading singularity of the solution of the integral equation is treated separately, while the more regular remainder is handled using graded-mesh quadratures, so that cancellations errors are eliminated and high order accuracy is achieved without recourse to highly refined submeshes. We demonstrate the efficacy of this algorithm through applications to solution of Neumann problems for the Laplace operator over a variety of domains—including domains containing extremely sharp concave and convex corners, with angles as small as $\pi/100$ and as large as $199\pi/100$.

The remainder of this paper is organized as follows: In Sect. 2, we introduce the PDE and associated second-kind integral equations, and we derive the leading asymptotics of the integral-equation solutions. Section 3 presents our method for treatment of the unbounded behavior of these solutions and the corresponding cancellation of infinities that occurs in the corresponding integral equations. In Sect. 4, in turn, we describe our discretization and solution methods. The difficulties mentioned in points

(1) and (2) above are demonstrated in Sect. 5. In Sect. 6, finally, we present several experiments which demonstrate the efficacy of our approach.

2 Integral equation formulations

2.1 Neumann problems

Let $\Omega \subset \mathbb{R}^2$ be an open, bounded domain, with a piecewise smooth Lipschitz boundary $\Gamma = \partial\Omega$. For clarity, we assume that the domain boundary $\partial\Omega$ contains a single corner point and is otherwise smooth; in particular, as shown in Fig. 1, the corner lies at the intersection of two smooth sub-arcs Γ_1 and Γ_2, which meet with an *interior angle* equal to $\alpha\pi$ for some $0 < \alpha < 2$, $\alpha \neq 1$. Throughout this paper the corner point is assumed to lie at the origin $x = \mathbf{0}$; the extension of our methods to problems containing multiple corners is straightforward.

We consider Neumann problems for the Laplace equation in interior and exterior domains with boundary Γ: for given Neumann data satisfying

$$\int_\Gamma g\, dS = 0 \tag{2.1}$$

and denoting by ν the outward unit normal, we seek solutions of the boundary value problems

$$\Delta u^{iN} = 0 \quad \text{in } \Omega, \quad \frac{\partial u^{iN}}{\partial \nu} = g \text{ on } \Gamma, \tag{2.2}$$

$$\Delta u^{eN} = 0 \quad \text{in } \mathbb{R}^2\backslash\overline{\Omega}, \quad \frac{\partial u^{eN}}{\partial \nu} = g \text{ on } \Gamma, \quad u^{eN}(x) = o(1) \text{ as } |x| \to \infty\,. \tag{2.3}$$

Remark 2.1 Throughout this paper we assume the Neumann data g is bounded, and of class C^m on $\Gamma\backslash\mathbf{0}$ with $m \geq 2$. Furthermore, we assume that $g \in C^m(\overline{\Gamma}_k)$, $k = 1, 2$.

The solution of the exterior problem is unique. The solution of the interior problem, in turn, is unique up to an additive constant; taking a point $x_0 \in \overline{\Omega}$ and a $\kappa \in \mathbb{R}$, we determine uniquely the solution of the interior Neumann problem by requiring

$$u^{iN}(x_0) = \kappa. \tag{2.4}$$

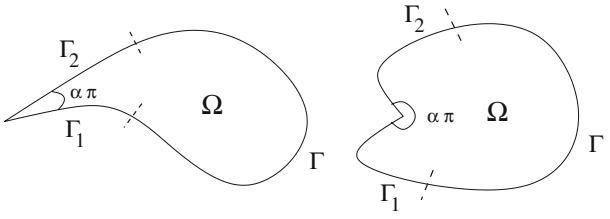

Fig. 1 Generic domains with acute and obtuse interior angles at the corner

2.2 Integral equations

Our algorithms for solution of these Neumann problems are based on use of the fundamental solution

$$G(x, y) = \frac{1}{2\pi} \ln \frac{1}{|x - y|},$$

representation formulae, and associated integral equations. For the interior Neumann problem, for example, we use the well known representation formula

$$u^{iN}(x) = \int_\Gamma G(x, y)\phi(y)\, dS(y) - \bar{u}^e \quad \text{for } x \in \Omega \quad \bar{u}^e = \int_\Gamma G(x_0, y)\phi(y)\, dS(y) - \kappa, \tag{2.5}$$

where the density ϕ satisfies the integral equation

$$\frac{\phi(x)}{2} + \int_\Gamma \frac{\partial G(x, y)}{\partial \nu(x)}\phi(y)\, dS(y) = g(x) \quad \text{for} \quad x \in \Gamma\backslash\{\mathbf{0}\}, \quad \int_\Gamma \phi(y)\, dS(y) = 0. \tag{2.6}$$

Analogously, for the solution u^{eN} of the exterior Neumann problem we use the representation formula

$$u^{eN}(x) = -\int_\Gamma G(x, y)\phi(y)\, dS(y) \quad \text{for } x \in \mathbb{R}\backslash\overline{\Omega}, \tag{2.7}$$

where ϕ satisfies the integral equation

$$\frac{\phi(x)}{2} - \int_\Gamma \frac{\partial G(x, y)}{\partial \nu(x)}\phi(y)\, dS(y) = g(x) \quad \text{for } x \in \Gamma\backslash\{\mathbf{0}\}, \quad \int_\Gamma \phi(y)\, dS(y) = 0. \tag{2.8}$$

As shown in [31,48], the integral equations (2.6) and (2.8) are uniquely solvable in $L_0^2(\Gamma) = \{\phi \in L^2(\Gamma) : \int_\Gamma \phi\, dS = 0\}$ where, of course, $L^2(\Gamma)$ is the space of square integrable functions on Γ.

2.3 Leading asymptotics

Following the presentation [54] we obtain the leading asymptotics of the solutions of Eqs. (2.6) and (2.8) near the corner; these asymptotic expressions are crucial components of our algorithms. To obtain the desired asymptotics we first note that, as shown

in [54] by consideration of the Green formulae, the solution of Eq. (2.8) is given by

$$\phi = g + \frac{\partial u^{iD}}{\partial \nu}$$

where u^{iD} is the unique solution of the complementary interior Dirichlet problem $\Delta u^{iD} = 0$ in Ω with boundary conditions $u^{iD} = -u^{eN}$ on Γ. Analogously, it is easy to show that the solution of Eq. (2.6) equals

$$\phi = g + \frac{\partial u^{eD}}{\partial \nu}$$

where u^{eD} is the unique solution of the exterior Dirichlet problem $\Delta u^{eD} = 0$ in $\mathbb{R}^2 \backslash \overline{\Omega}$ with $u^{eD} = -u^{iN}$ on Γ and u^{eD} bounded at infinity.

Clearly, the leading asymptotics of the solutions ϕ of Eqs. (2.6) and (2.8) are determined by the corresponding asymptotics of the normal derivative of the solution of the complementary Dirichlet problems. The asymptotic behavior of solutions of Dirichlet and Neumann problems in domains with corners is discussed in a wide range of contributions, including [11,14,23,24,39,34,49–51,54]; the references [11,33,49,54] are particularly relevant in the present context since, like the present work, they *do not assume* that Γ coincides with a pair of straight segments near the corner. Letting $r = |x|$ be the distance to the corner, in what follows we consider the asymptotics of the relevant Dirichlet problems in corner-type domains for which the Γ_1 and Γ_2 are general smooth curves (not necessarily straight segments), and we thus determine the asymptotic behavior as $r \to 0$ of the solution ϕ: we obtain (see also [54])

(INA) Interior Neumann problem, Acute angle ($0 < \alpha < 1$): for some constant a, $\phi = a r^{\frac{1}{2-\alpha}-1} + o(1)$.

(INO) Interior Neumann problem, Obtuse angle ($1 < \alpha < 2$): for some constant a, $\phi = \pm a r^{\frac{1}{\alpha}-1} + o(1)$, where the $+$ (respectively $-$) sign gives the asymptotics as x approaches the corner along Γ_1 (resp. Γ_2); see Fig. 1.

(ENA) Exterior Neumann problem, Acute angle ($0 < \alpha < 1$): for some constant a, $\phi = \pm a r^{\frac{1}{2-\alpha}-1} + o(1)$, where the $+$ (respectively $-$) sign gives the asymptotics as x approaches the corner along Γ_1 (resp. Γ_2); see Fig. 1.

(ENO) Exterior Neumann problem, Obtuse angle ($1 < \alpha < 2$): for some constant a, $\phi = a r^{\frac{1}{\alpha}-1} + o(1)$.

Remark 2.2 Note that, in each one of these cases, the solutions ϕ of the integral equations (2.6) and (2.8) blow up as $r \to 0$ along Γ, a fact that was recognized at least as early as 1949 [39].

In order to keep the presentation self-contained, and to provide necessary details that were absent from previous presentations for cases in which Γ_1 and Γ_2 are arbitrary smooth arcs, in what follows we present proofs of these facts. We thus establish the asymptotic relations (INA) and (INO) on the basis of the previous results [49, Theorem 3.1 and Theorem 3.3] on PDE solution asymptotics; the particular cases of

those theorems that are needed in our context are stated below as Theorem 2.3. The relations (ENA) and (ENO) follow similarly.

Theorem 2.3 *Let D be an open set in the $z = x_1 + i x_2$ plane, part of whose boundary consists of two analytic arcs Γ_1 and Γ_2, which meet at the origin, where they form an angle $\beta\pi > 0$ (interior to D). We assume that Γ_j ($j = 1, 2$) is an open arc of an analytic curve of which the origin is a regular point. Let $m \geq 2$ be an integer. Let $u(x_1, x_2) = u(z)$ satisfy $\Delta u = f$ in D, where f is of class C^m in $D \cup \Gamma_1 \cup \Gamma_2 \cup \{\mathbf{0}\}$; and let g_i be a function of arc length which is of class C^m on $\Gamma_j \cup \{\mathbf{0}\}$, $j = 1, 2$.*

Dirichlet case: Suppose that $u = g_j$ on Γ_j, $j = 1, 2$. Then for $z \to 0$, $z \in D \cup \Gamma_1 \cup \Gamma_2$, $u(z)$ has an asymptotic expansion

$$u(z) = \log z\, Q_1 + \log \bar{z}\, Q_2 + Q_3 + o(z^{m-\epsilon}) \quad \text{for any } \epsilon > 0,$$

where Q_1, Q_2 and Q_3 are polynomials in z, $\bar{z}$, $z^{1/\beta}$ and $\bar{z}^{1/\beta}$ if β is irrational, and in z, $\bar{z}$, $z^{1/\beta}$, $\bar{z}^{1/\beta}$, $z^q \log z$ and $\bar{z}^q \log \bar{z}$ if $\beta = p/q$, $(p, q) = 1$. If $g_1(0) = g_2(0)$, then Q_1 and Q_2 vanish identically. Furthermore, expansions for derivatives of $u(z)$ of order $\leq m - 1$ may be obtained by differentiating formally.

Neumann case: Suppose that $\partial u/\partial \nu = g_j$ on Γ_j, $j = 1, 2$. Then for $z \to 0$, $z \in D \cup \Gamma_1 \cup \Gamma_2$, $u(z)$ has an asymptotic expansion

$$u(z) = \log z\, Q_1 + \log \bar{z}\, Q_2 + Q_3 + o(z^{m+1-\epsilon}) \quad \text{for any } \epsilon > 0,$$

where Q_1, Q_2 and Q_3 are polynomials in z, $\bar{z}$, $z^{1/\beta}$ and $\bar{z}^{1/\beta}$ if β is irrational, and in z, $\bar{z}$, $z^{1/\beta}$, $\bar{z}^{1/\beta}$, $z^q \log z$ and $\bar{z}^q \log \bar{z}$ if $\beta = p/q$, $(p, q) = 1$. If $u(z)$ is bounded at the origin, then Q_1 and Q_2 vanish identically. Furthermore, expansions for derivatives of $u(z)$ of order $\leq m$ may be obtained by differentiating formally.

To establish (INA) and (INO) we first show that the solution u^{iN} of Eq. (2.2) is bounded, for which, in turn, we consider the solution v^{iD} of the Dirichlet problem conjugate to Eq. (2.2) in Ω—see [32, pp. 102–103, probs. 6,8]. The boundary values of v^{iD} equal an integral (primitive) $\hat{g}$ of g along the boundary Γ; note that, importantly, in view of Eq. (2.1) $\hat{g}$ is continuous at the corner. We deduce from the Dirichlet case of Theorem 2.3 that v^{iD} is bounded, and that its leading asymptotic behavior is given by

$$v^{iD} = const. + r^{1/\alpha}(c_1 \cos(\theta/\alpha) + c_2 \sin(\theta/\alpha)) + O(r^{\min\{2/\alpha, 2\}-\epsilon}), \tag{2.9}$$

where ϵ is an arbitrarily small positive number. Taking an arbitrary point $\bar{x} \in \Omega$, because of the conjugacy relationship between u^{iN} and v^{iD}, for all $x \in \Omega$ we have

$$u^{iN}(x) = u^{iN}(\bar{x}) + \int_{\bar{x}}^{x} (v^{iD}_{x_1}\, dx_2 - v^{iD}_{x_2}\, dx_1), \tag{2.10}$$

where the integral can follow any path in Ω between $\bar{x}$ and x. In view of the fact that the asymptotics (Eq. 2.9) can be formally differentiated, the integrand in Eq. (2.10)

is bounded by r^γ for some $\gamma > -1$ and is thus uniformly integrable for x in the closure of Ω. It follows easily that u^{iN} is bounded, as claimed. Having established the boundedness of u^{iN}, we conclude from the Neumann case of Theorem 2.3 that, for any $\epsilon > 0$, as $x \to 0$

$$u^{iN}(x) = u^{iN}(x_1, x_2) = \Re(P_m(z) + R_m(z)), \tag{2.11}$$

where P_m is either a polynomial in $\{z, \bar{z}, z^{1/\alpha}, \bar{z}^{1/\alpha}\}$ (if $\alpha \in \mathbb{I} = \mathbb{R}\backslash\mathbb{Q}$), or a polynomial in $\{z, \bar{z}, z^{1/\alpha}, \bar{z}^{1/\alpha}, z^q \ln z, \bar{z}^q \ln \bar{z}\}$ (if $\alpha = p/q \in \mathbb{Q}$, $(p, q) = 1$), and where $|R_m(z)| = o(z^{m+1-\epsilon})$.

Recalling that the solution u^{eD} of the complementary exterior Dirichlet problem has boundary values $u^{eD} = -u^{iN}$, we seek to obtain the needed asymptotics of u^{eD} via an application of the Dirichlet case of Theorem 2.3. To take advantage of this result, however, we must at first address the fact that the boundary values of $-u^{iN}$ do not satisfy the smoothness assumptions of this theorem. To do this we assume, without loss of generality, that, at the origin, Γ_1 and Γ_2 are tangent to the rays $\theta = 0$ and $\theta = \alpha\pi$, respectively. And, further, we show that, in the present context, (2.11) may be re-expressed as

$$u^{iN} = u_1^{iN} + u_2^{iN} \tag{2.12}$$

where $u_2^{iN} \in C^2(\overline{\Gamma}_j)$, $j = 1, 2$, and where u_1^{iN} is given by an expression of the form

$$\begin{aligned} u_1^{iN} = &\sum_{k=1}^{3} c_{1k}\, r^{k/\alpha} \cos\frac{k\theta}{\alpha} + c_2\, r^2(\ln r\, \cos 2\theta - \theta\, \sin 2\theta) \\ &+ r^{1+1/\alpha}\left(c_3 \sin\frac{(1+\alpha)\theta}{\alpha} + c_4\, \cos\frac{(1+\alpha)\theta}{\alpha}\right). \end{aligned} \tag{2.13}$$

In order to establish Eq. (2.12) from Eq. (2.11) we note that u^{iN} cannot contain a term of the form $r^{1/\alpha} \sin\frac{\theta}{\alpha}$, since, as is easily checked, such a term would require the Neumann data $g = \frac{\partial u^{iN}}{\partial \nu}$ to be unbounded at the corner. Terms corresponding to the imaginary parts of $\{z^{2/\alpha}, z^{3/\alpha}, z^{1+1/\alpha}, z^2 \ln z\}$—their real parts are represented in u_1^{iN}—can be seen to be of class C^2 on $\overline{\Gamma}_j$, $j = 1, 2$, so they are included in u_2^{iN}. We note, further, that the terms of the form $\mathcal{A} = \{|z|^{2/\alpha}, z\bar{z}^{1/\alpha}, z^{2/\alpha}\bar{z}^{1/\alpha}\}$ cannot be part of u_1^{iN} since, depending on the specific values of α, these terms are either smooth (and must thus be included in u_2^{iN}) or they have an unbounded Laplacian (and thus cannot be part of Eq. (2.11) in the first place). Note, finally, that the coefficient c_2 can only be non-zero when α is rational and satisfies $0 < \alpha < 2$ and $\alpha \neq 1$—that is, $\alpha = 1/2$ or $\alpha = 3/2$.

Having determined the singular part u_1^{iN} of u^{iN}, we let χ be a smooth cutoff function which is identically 1 in a neighborhood of the origin and vanishes outside some disc, and we construct a function u_1^{eD} which is harmonic in $\mathbb{R}^2\backslash\overline{\Omega}$, such that $u_1^{iN} + \chi u_1^{eD}$, and hence $u^{iN} + \chi u_1^{eD}$, is of class C^2 on $\overline{\Gamma}_j$, $j = 1, 2$—this is what is needed to determine the asymptotic behavior of $u^{eD} = \chi u_1^{eD} + u_2^{eD}$ via Theorem 2.3. One can

verify by direct computation that u_1^{eD} given by

$$
\begin{aligned}
-u_1^{eD} = &\sum_{k=1}^{3} c_{1k}\ \sec\frac{k\pi}{\alpha}\, r^{k/\alpha}\cos\frac{k(\theta-\pi)}{\alpha} + c_2\, r^2(\ln r\ \cos 2\theta - \theta\ \sin 2\theta) \\
&+ r^{1+1/\alpha}\left(c_3\,\frac{\sin\alpha\pi}{\sin\frac{(\alpha-2)\pi}{\alpha}}\ \sin\frac{(1+\alpha)\theta-2\pi}{\alpha} \right. \\
&\left. + c_4\ \sec\left(\frac{2\pi}{\alpha}-\bar\theta\right)\cos\left(\frac{(1+\alpha)\theta}{\alpha}-\bar\theta\right)\right),
\end{aligned}
\tag{2.14}
$$

where $\bar\theta = \operatorname{arccot}(\cot(\pi/\alpha) - \csc^2(\pi/\alpha)\tan(\alpha\pi)/2)$, satisfies our requirements. Here, the coefficients $\{c_{11}, c_{12}, c_{13}, c_2, c_3, c_4\}$ are precisely those in Eq. (2.13). We now apply Theorem 2.3 to the function u_2^{eD}, satisfying $\Delta u_2^{eD} = -\Delta(\chi u_1^{eD})$ in $\mathbb{R}^2\backslash\overline{\Omega}$ and $u_2^{eD} = -(u^{iN} + \chi\tilde u_1^{eD})$ on Γ. We deduce that, as $z \to 0$,

$$
u_2^{eD}(x) = \Re(\tilde P_2(z) + \tilde R_2(z)),
\tag{2.15}
$$

where $\tilde P_2$ is a polynomial in either $\{z, \bar z, z^{1/(2-\alpha)}, \bar z^{1/(2-\alpha)}\}$ or $\{z, \bar z, z^{1/(2-\alpha)}, \bar z^{1/(2-\alpha)}, z^q \ln z, \bar z^q \ln \bar z\}$ under the $\mathbb{I}/\mathbb{Q}$ criterion given above, and $|\tilde R_2(z)| = o(z^{2-\epsilon})$ for any $\epsilon > 0$.

From this discussion we determine that, in a neighborhood of the origin, u^{eD} has the form

$$
u^{eD}(x) = a_0 + r^{1/(2-\alpha)}\left(a_1 \sin\tfrac{\theta-2\pi}{2-\alpha} + a_2\cos\tfrac{\theta-2\pi}{2-\alpha}\right) + a_3\, x_1 + a_4\, x_2 + o(r)
\tag{2.16}
$$

for $0 < \alpha < 1$, and

$$
u^{eD}(x) = a_0 + a_1\, r^{1/\alpha}\cos\tfrac{\theta-\pi}{\alpha} + a_2\, x_1 + a_3\, x_2 + o(r)
\tag{2.17}
$$

for $1 < \alpha < 2$. Therefore, when $0 < \alpha < 1$,

$$
\tfrac{\partial u^{eD}}{\partial \nu} \sim -\tfrac{a_1}{2-\alpha}\, r^{1/(2-\alpha)-1} \quad \text{as } x \to 0 \text{ along } \Gamma_1 \text{ or } \Gamma_2.
\tag{2.18}
$$

When $1 < \alpha < 2$, we have

$$
\frac{\partial u^{eD}}{\partial \nu} \sim \frac{a_1\ \sin(\pi/\alpha)}{\alpha}\, r^{1/\alpha-1} \text{ as } x \to 0 \text{ along } \Gamma_1 \quad \text{and}
\tag{2.19}
$$

$$
\frac{\partial u^{eD}}{\partial \nu} \sim -\frac{a_1\ \sin(\pi/\alpha)}{\alpha}\, r^{1/\alpha-1} \text{ as } x \to 0 \text{ along } \Gamma_2.
\tag{2.20}
$$

Relations (2.18)–(2.20) establish the leading behavior claimed for the solutions ϕ of Eqs. (2.6) and (2.8) in (INA) and (INO). The $o(1)$ behavior of the remainder is based

on the fact that the linear terms in u^{iN} and u^{eD} differ only by sign near the origin due to the Dirichlet boundary conditions, so the constant in $\phi = \frac{\partial u^{iN}}{\partial \nu} + \frac{\partial u^{eD}}{\partial \nu}$ vanishes, leaving an $o(1)$ remainder.

Parametrization. In what follows we use parametrized versions of the integral equations (2.6) and (2.8). To do this we use a smooth parameterization $x = x(t)$ of Γ with $x(0) = x(T) = \mathbf{0}$, and we assume $x(t)$ traverses Γ in a counter-clockwise fashion with strictly positive speed, $|x'(t)| \geq s_0 > 0$. Then the integral equations for the interior and exterior Neumann problems, Eqs. (2.6) and (2.8), are expressed, respectively, as

$$\frac{\mu(t)}{2} - \int_0^T K(t,s)\mu(s)\,ds = f(t), \quad \int_0^T \mu(s)|x'(s)|\,ds = 0, \quad \text{and} \tag{2.21}$$

$$\frac{\mu(t)}{2} + \int_0^T K(t,s)\mu(s)\,ds = f(t), \quad \int_0^T \mu(s)|x'(s)|\,ds = 0, \tag{2.22}$$

where

$$\begin{aligned} K(t,s) &= \frac{(x(t)-x(s))\cdot n(t)}{2\pi|x(t)-x(s)|^2}\,|x'(s)|, \qquad n(t) = \nu(x(t)) \\ f(t) &= g(x(t)), \qquad\qquad\qquad\qquad\quad \mu(t) = \phi(x(t)). \end{aligned} \tag{2.23}$$

We note that for $s = t$ we have $K(t,t) = -x''(t)\cdot n(t)/(4\pi|x'(t)|)$; as is well-known, the kernel K is of class C^∞ for $s, t \in (0,T)$. For x of class $C^{m+2}[0,T]$ (a case that can be treated with no difficulty by the algorithm introduced in this paper), then K is of class C^m for $s, t \in (0,T)$. For definiteness, however, we assume throughout that both x and the Neumann data f are smooth: $x \in (C^\infty[0,T])^2$ and $f \in C^\infty[0,T]$.

3 Stable evaluation of cancellations

We describe our numerical method for the interior problem (2.21); the corresponding exterior problem (2.22) can be treated similarly.

3.1 Cancellation of infinities and leading solution asymptotics

The essence of our method resides in use of the asymptotics (INA) and (INO) (or (ENA) and (ENO) for the exterior problems) to resolve the difficulties detailed in Sect. 5, namely indeterminate limits and subtractive cancellation, as well as inaccurate Nyström integration. In this section, we provide a method that successfully tackles the first of these difficulties.

Remark 3.1 Note that cancellation of infinities does indeed occur in Eqs. (2.21)–(2.22) since, generically, μ tends to infinity at the corner and the right-hand side of

these equations is finite. A numerical example demonstrating the need for a special numerical treatment of this problem is provided in Table (2): high accuracy may not be expected in general unless this issue is satisfactorily addressed.

To resolve the indeterminate limit mentioned above we first re-express the integral equation solutions to explicitly account for the asymptotics (INA) and (INO): we write

$$\mu(t) = a\mu_1(t) + \mu_2(t), \quad \mu_1(t) = \psi(t)|x(t)|^{-q}, \quad q = \begin{cases} 1 - \frac{1}{2-\alpha}, & 0 < \alpha < 1 \\ 1 - \frac{1}{\alpha}, & 1 < \alpha < 2 \end{cases}, \tag{3.1}$$

where ψ is a smooth real-valued function for $0 \le t \le T$ satisfying, for certain appropriately selected values R and S, $0 < R < S < T$,

$$\psi(t) = \begin{cases} 1 \quad \text{for } t \in [0, R] \cup [S, T] \text{ when } 0 < \alpha < 1, \text{ and} \\ \begin{bmatrix} -1 & \text{for } t \in [0, R] \\ 1 & \text{for } t \in [S, T] \end{bmatrix} \quad \text{when } 1 < \alpha < 2, \end{cases}$$

and where μ_2 is a Hölder continuous function [49] *that vanishes at* $t = 0$ *and* $t = T$. The unknowns in our problem thus become the parameter $a \in \mathbb{R}$ and the function μ_2. In our implementation we use $\psi \equiv 1$ when $0 < \alpha < 1$, and

$$\psi(t) = 2\,\frac{e^{-1/(t-R)}}{e^{-1/(t-R)} + e^{-1/(S-t)}} - 1 \text{ for } t \in (R, S) \tag{3.2}$$

when $1 < \alpha < 2$. The interior Neumann problem (2.21) can now be expressed as

$$\frac{\mu_2(t)}{2} - \int_0^T K(t, s)\mu_2(s)\,ds + af_1(t) = f(t), \quad \int_0^T |x'(s)|\mu_2(s)\,ds + az_1 = 0, \tag{3.3}$$

where

$$f_1(t) = \frac{\mu_1(t)}{2} - \int_0^T K(t, s)\mu_1(s)\,ds \quad \text{and} \quad z_1 = \int_0^T |x'(s)|\mu_1(s)\,ds. \tag{3.4}$$

Remark 3.2 The infinity cancellation mentioned in Remark 3.1 is encapsulated in the function f_1 in (3.4)—since the function μ_2 is Hölder continuous and vanishes at $t = 0$ and $t = T$, and, thus, all other terms in Eq. (3.3) are bounded for $t \in [0, T]$. It follows, in particular, that the function $f_1(t)$ is itself bounded for $t \in [0, T]$.

3.2 Stable evaluation of indeterminate limits: a canonical problem

The difficulties arising from cancellations of infinities can be addressed by resolving analytically the indeterminate limits $\lim_{t\to 0} f_1(t)$ and $\lim_{t\to T} f_1(t)$. To do this, we

first introduce approximations L_1 and L_2 of the kernel K around the endpoints 0 and T,

$$L_1(t,s) = \frac{(tx'(0) - (s-T)x'(T)) \cdot n(0)\,|x'(T)|}{2\pi\,|tx'(0) - (s-T)x'(T)|^2} = \frac{\sin(\alpha\pi)\,|(s-T)x'(T)|\,|x'(T)|}{2\pi\,|tx'(0) - (s-T)x'(T)|^2} \tag{3.5}$$

$$L_2(t,s) = \frac{((t-T)x'(T) - sx'(0)) \cdot n(T)\,|x'(0)|}{2\pi\,|(t-T)x'(T) - sx'(0)|^2} = \frac{\sin(\alpha\pi)\,|sx'(0)|\,|x'(0)|}{2\pi\,|(t-T)x'(T) - sx'(0)|^2}. \tag{3.6}$$

and the associated quantities

$$\sigma_1(t) = \psi(0)\,\frac{|tx'(0)|^{-q}}{2} - \int_S^T L_1(t,s)|(s-T)x'(T)|^{-q}\,ds \tag{3.7}$$

$$\sigma_2(t) = \frac{|(t-T)x'(T)|^{-q}}{2} - \psi(0)\int_0^R L_2(t,s)|sx'(0)|^{-q}\,ds. \tag{3.8}$$

Remark 3.3 If Γ_1 and Γ_2 are straight segments parametrized by linear functions with speeds $x'(0)$ and $x'(T)$, then $L_1(t,s) = K(t,s)$ for t near 0 and s near T, and $L_2(t,s) = K(t,s)$ for t near T and s near 0. The quantities σ_1 and σ_2, which themselves give rise to cancellation of infinities as $t \to 0$ and $t \to T$, capture the essence of the cancellations inherent in the quantity $f_1(t)$.

The key to our algorithm lies in recognizing that σ_1 and σ_2 can be evaluated as rapidly converging series expansions, thereby providing, via the simple additional manipulations described in Sect. 3.2.2, an efficient and numerically stable means for evaluation of the quantity $f_1(t)$ in and around $t = 0$ and $t = T$.

3.2.1 Series expansions for σ_1 and σ_2

Introducing the notations

$$V_1 = (T-S)|x'(T)| \qquad V_2 = R|x'(0)|$$

$$B_1(t) = \frac{t\,|x'(0)|}{V_1} \qquad B_2(t) = \frac{(T-t)\,|x'(T)|}{V_2}$$

together with the parameters $0 < \hat{S} < \hat{R} < T$, which are selected in such a way that $B_1(t) \le 1$ for $t \le \hat{S}$, and $B_2(t) \le 1$ for $t \ge \hat{R}$, we have the following series

expansions for the functions σ_1 and σ_2:

$$\sigma_1(t) = \psi(0)\,\frac{V_1^{-q}}{2\pi}\sum_{k=1}^{\infty}\frac{\sin(k\alpha\pi)}{k+q-1}[B_1(t)]^{k-1} \quad \text{for } t\in(0,\hat{S}] \tag{3.9}$$

$$\sigma_2(t) = \frac{V_2^{-q}}{2\pi}\sum_{k=1}^{\infty}\frac{\sin(k\alpha\pi)}{k+q-1}[B_2(t)]^{k-1} \quad \text{for } t\in[\hat{R},T). \tag{3.10}$$

In particular, σ_1 and σ_2 are analytic functions on their domains of definition. We can, in fact, establish a somewhat more general result for the related functions

$$\sigma_1^{\pm}(t,\lambda) = \frac{|tx'(0)|^{\lambda}}{2} \pm \int_S^T L_1(t,s)|(s-T)x'(T)|^{\lambda}\,ds,$$

$$\sigma_2^{\pm}(t,\lambda) = \frac{|(t-T)x'(T)|^{\lambda}}{2} \pm \int_0^R L_2(t,s)|sx'(0)|^{\lambda}\,ds.$$

Lemma 3.4 *Let $-1<\lambda<0$ be given. For $t\in(0,\hat{S}]$, we have*

$$\sigma_1^{\pm}(t,\lambda) = \left(1\pm\frac{\sin(\lambda\pi-(1+\lambda)\alpha\pi)}{\sin(\lambda\pi)}\right)\frac{|tx'(0)|^{\lambda}}{2} \mp \frac{V_1^{\lambda}}{2\pi}\sum_{k=1}^{\infty}\frac{\sin(k\alpha\pi)}{k-\lambda-1}[B_1(t)]^{k-1}. \tag{3.11}$$

An analogous expansion holds for $\sigma_2^{\pm}$ in the domain $t\in[\hat{R},T)$, namely

$$\sigma_2^{\pm}(t,\lambda) = \left(1\pm\frac{\sin(\lambda\pi-(1+\lambda)\alpha\pi)}{\sin(\lambda\pi)}\right)\frac{|(T-t)x'(T)|^{\lambda}}{2} \mp\frac{V_2^{\lambda}}{2\pi}\sum_{k=1}^{\infty}\frac{\sin(k\alpha\pi)}{k-\lambda-1}[B_2(t)]^{k-1}. \tag{3.12}$$

Proof The proof is given for $\sigma_1^{\pm}$. We have

$$\begin{aligned}
\sigma_1^{\pm}(t,\lambda) &= \frac{|tx'(0)|^{\lambda}}{2\pi}\left(\pi\pm\int_0^{[B_1(t)]^{-1}}\frac{\sin(\alpha\pi)v^{1+\lambda}}{1-2\cos(\alpha\pi)v+v^2}\,dv\right)\\
&= \frac{|tx'(0)|^{\lambda}}{2\pi}\left(\pi\pm\int_0^{1}\frac{\sin(\alpha\pi)v^{1+\lambda}}{1-2\cos(\alpha\pi)v+v^2}\,dv\pm\int_{B_1(t)}^{1}\frac{\sin(\alpha\pi)w^{-(1+\lambda)}}{1-2\cos(\alpha\pi)w+w^2}\,dw\right)\\
&= \frac{|tx'(0)|^{\lambda}}{2\pi}\left(\pi\pm\sum_{k=1}^{\infty}\int_0^{1}\sin(k\alpha\pi)v^{k+\lambda}\,dv\pm\sum_{k=1}^{\infty}\int_{B_1(t)}^{1}\sin(k\alpha\pi)w^{k-\lambda-2}\,dw\right)
\end{aligned}$$

$$= \frac{|tx'(0)|^\lambda}{2\pi}\left(\pi \pm \sum_{k=1}^{\infty} \frac{2k\,\sin(k\alpha\pi)}{k^2-(\lambda+1)^2}\right) \mp \frac{V_1^\lambda}{2\pi}\sum_{k=1}^{\infty}\frac{\sin(k\alpha\pi)}{k-(\lambda+1)}[B_1(t)]^{k-1}$$

$$= \frac{|tx'(0)|^\lambda}{2}\left(1 \pm \frac{\sin(\lambda\pi-(1+\lambda)\alpha\pi)}{\sin(\lambda\pi)}\right) \mp \frac{V_1^\lambda}{2\pi}\sum_{k=1}^{\infty}\frac{\sin(k\alpha\pi)}{k-(\lambda+1)}[B_1(t)]^{k-1}.$$

The changes-of-variables, $s = T - \frac{|tx'(0)|}{|x'(T)|}v$ and $v = w^{-1}$ yield the first two identities; the conversion of the integrands to series follows by expansion of the corresponding integrands. The proof is completed by noting that the Fourier series of $\pi\sin(\lambda\pi-(1+\lambda)\theta)\csc(\lambda\pi)$ is a sine series with coefficients $2k/(k^2-(\lambda+1)^2)$.

Remark 3.5 In light of the facts that, $\sigma_1(t) = \sigma_1^-(t,-q)$ and $\sigma_2(t) = \sigma_2^-(t,-q)$ for $0 < \alpha < 1$, while $\sigma_1(t) = -\sigma_1^+(t,-q)$ and $\sigma_2(t) = \sigma_2^+(t,-q)$, for $1 < \alpha < 2$, the relations (3.9) and (3.10) follow directly from the previous lemma—since, for $\lambda = -q$ [with q given by Eq. (3.1)], the coefficient of $|tx'(0)|^\lambda$ in Eq. (3.11) vanishes. Furthermore, $-q$ is the only value of $\lambda \in (-1, 0)$ for which this coefficient vanishes.

3.2.2 *Resolution of the infinity cancellations in* $f_1(t)$

When $t \in (\hat{S}, \hat{R})$—sufficiently far from both 0 and T—no special treatment is needed to evaluate $f_1(t)$ accurately, and we do so by direct integration and subtraction as indicated in Eq. (3.4). For $t \in [0, \hat{S}] \cup [\hat{R}, T]$, our method for stable evaluation of $f_1(t)$ involves the computation of $\sigma_1(t)$ or $\sigma_2(t)$ via series expansions, and the evaluation of certain singular integrals (that, as detailed in Sect. 4, are treated with high-order accuracy by previously existing methods and generalizations thereof presented in Appendix A) together with some simple algebraic manipulations. To evaluate $f_1(t)$ we thus define

$$E_1(t,s) = L_1(t,s)|x'(T)|^{-q} - K(t,s)\left|\frac{x(s)}{s-T}\right|^{-q} \tag{3.13}$$

$$\eta_1(t) = \psi(0)\,\frac{|x(t)|^{-q} - |tx'(0)|^{-q}}{2} = \psi(0)\left(\left|\frac{x(t)}{t}\right|^{-q} - |x'(0)|^{-q}\right)\frac{t^{-q}}{2} \tag{3.14}$$

$$E_2(t,s) = \psi(0)\left(L_2(t,s)|x'(0)|^{-q} - K(t,s)\left|\frac{x(s)}{s}\right|^{-q}\right) \quad \text{and} \tag{3.15}$$

$$\eta_2(t) = \frac{|x(t)|^{-q} - |(t-T)x'(T)|^{-q}}{2} = \left(\left|\frac{x(t)}{t-T}\right|^{-q} - |x'(T)|^{-q}\right)\frac{(T-t)^{-q}}{2} \tag{3.16}$$

and we employ two different expressions for $f_1(t)$ near the corner, namely

$$f_1(t) = \eta_1(t) + \sigma_1(t) - \int_0^S K(t,s)\mu_1(s)\,ds + \int_S^T E_1(t,s)(T-s)^{-q}\,ds, \quad (3.17)$$

and

$$f_1(t) = \eta_2(t) + \sigma_2(t) - \int_R^T K(t,s)\mu_1(s)\,ds + \int_0^R E_2(t,s)s^{-q}\,ds; \quad (3.18)$$

the first expression is used for $t \in [0, \hat{S}]$ while the second is used for $t \in [\hat{R}, T]$.

To verify that these expressions adequately resolve the indeterminate limits inherent in Eq. (3.4) (and hence Eq. (2.21)), we show that each of the components in Eqs. (3.17) and (3.18) are bounded as $t \to 0$ and $t \to T$, respectively. We restrict our discussion to Eq. (3.17); the considerations concerning Eq. (3.18) are analogous. To show that the various terms in Eq. (3.17) are bounded as $t \to 0$, we first recall the results of Sect. 3.2.1, from which it follows directly that $\sigma_1(t)$ is bounded. Further, it is easy to check from Eq. (3.14) that $\eta_1(t)$ is bounded on $[0, \hat{S}]$; the integral with the kernel $K(t,s)$ in Eq. (3.17), in turn, is clearly bounded since K is continuous for $t, s \in [0, \hat{S}]$. Since, as pointed out in Remark 3.2, the function $f_1(t)$ itself is bounded for $t \in [0, T]$, it follows that the integral with kernel $E_1(t,s)$ must be bounded as well: as claimed, each one of the individual terms in Eq. (3.17) are bounded as $t \to 0$.

The quantities $\eta_1(t)$, $\eta_2(t)$ can be computed directly using the expressions (3.14) and (3.16) for t sufficiently far from 0 and T. In order to avoid cancellation errors, in turn, for t close to 0 in our algorithm for evaluation of $\eta_1(t)$ we use a few terms of the Taylor expansion of the quantity in parenthesis on the right-hand expression of Eq. (3.14); similarly, a Taylor expansion is used to evaluate $\eta_2(t)$ for t close to T. In Appendix A we describe our treatment of the cancellation in the kernels E_1 and E_2, which is also based on use of Taylor series expansions.

4 Numerical implementation

Having re-expressed the integral equation (2.21) in the form (Eq. 3.3), and having obtained expressions that resolve the cancellations inherent in the function f_1, we are now ready to describe our overall discretization and solution process for Eq. (2.21). Recall that the unknown density is given by $\mu(t) = a\mu_1(t) + \mu_2(t)$, where the *known* leading singularity is encapsulated in $\mu_1(t)$, and the unknowns are the coefficient a and the Hölder function $\mu_2(t)$. As the action of the integral operators can be treated with high-order accuracy by means of previously existing quadrature rules for functions which, like $\mu_2(t)$, are Hölder continuous and vanish at $t = 0$ and $t = T$ (cf. [2,22,36]), the key to our approach lies in using efficient high-order methods for evaluation of $f_1(t) = \mu_1(t)/2 - \int_0^T K(t,s)\mu_1(s)\,ds$ for all $t \in [0, T]$, and $z_1 = \int_0^T |x'(s)|\mu_1(s)\,ds$.

We first describe the overall Nyström method, and then return to the computation of $f_1(t)$ and z_1.

4.1 The Nyström linear system

For integration of uniformly integrable functions, our implementation uses the quadrature rule introduced in [36], which, for completeness, is described in Appendix A. Denoting the corresponding quadrature points and weights by $t_k \in (0, T)$ and w_k, $1 \le k \le M$, respectively, our linear system is given by

$$\tilde{f}_1(0)\,\tilde{a} + \frac{\tilde{\mu}_0}{2} - \sum_{j=1}^{M} K(0, t_j) w_j\,\tilde{\mu}_j = f(0) \tag{4.1}$$

$$\tilde{f}_1(t_i)\,\tilde{a} + \frac{\tilde{\mu}_i}{2} - \sum_{j=1}^{M} K(t_i, t_j) w_j\,\tilde{\mu}_j = f(t_i),\ 1 \le i \le M \tag{4.2}$$

$$\tilde{f}_1(T)\,\tilde{a} + \frac{\tilde{\mu}_T}{2} - \sum_{j=1}^{M} K(T, t_j) w_j\,\tilde{\mu}_j = f(T) \tag{4.3}$$

$$\tilde{z}_1\,\tilde{a} + \sum_{j=1}^{M} |x'(t_j)|\, w_j\,\tilde{\mu}_j = 0 \tag{4.4}$$

$$\tilde{\mu}_0 = \tilde{\mu}_T = 0, \tag{4.5}$$

where $\tilde{f}_1(t)$ and $\tilde{z}_1$ are approximations (whose evaluation is described below) of $f_1(t)$ and z_1, and where $\tilde{a}$, $\tilde{\mu}_k$, $\tilde{\mu}_0$ and $\tilde{\mu}_T$ are (unknown) numerical approximations of a, $\mu_2(t_k)$, $\mu_2(0) = 0$, and $\mu_2(T) = 0$, respectively.

Clearly, this system contains $M + 5$ equations and $M + 3$ unknowns: it is slightly overdetermined. Our experience has shown that this over-determined system is significantly better conditioned than the square system obtained from Eqs. (4.2) and (4.4) by removing $\tilde{\mu}_0$ and $\tilde{\mu}_T$. Further, we have noticed that, for mild angles, no significant improvements arise from use of the additional equations (4.5); in such cases we do eliminate $\tilde{\mu}_0,\ \tilde{\mu}_t$ before solving the system (which still is overdetermined). For sharp angles, in contrast, we do not eliminate these equations, as our experiments have shown that incorporating Eq. (4.5) improves performance. In either case, we solve the over-determined system in the least-squares sense, by means of the well known QR-based least square solver. We note that, if desired, iterative least square solvers [6] could be used in conjunction with accelerated formulations of our algorithm.

4.2 Evaluation of $f_1(t)$ and z_1

To evaluate integrals with integrands given by "a smooth function multiplied by a singular function known in closed form"—namely z_1 and the integral that is part of $f_1(t)$ for $t \in (\hat{S}, \hat{R})$—we use quadratures that exploit the special form of the integrand. Although specialized Gaussian quadratures could be used for this purpose,

we prefer the flexibility of Clenshaw–Curtis-type quadratures, which we describe in Appendix A.2. To complete the evaluation of f_1 we need to provide an algorithm for values of t close to 0 and T; we do this, naturally, by exploiting the expressions (3.17) and (3.18). We summarize the elements in the computation of $f_1(t)$ for $t \in [0, \hat{S}]$; analogous procedures are used for $t \in [\hat{R}, T]$. For a given $t \in (0, \hat{S}]$, our algorithm consists of the following steps:

1. Evaluate $\sigma_1(t)$ by adding the first few terms of the series (Eq. 3.9). In practice, we choose $\hat{S}$ so that $B_1(t) \leq 1/2$ for $t \in [0, \hat{S}]$. This choice, though not necessary, guarantees rapid convergence of the series: use of twenty terms of the expansion is more than sufficient for all the experiments reported in this paper. In all experiments we have chosen $R = T - S = 0.1$ and $\hat{S} = T - \hat{R} = 0.05$; see Sect. 3.2.1.
2. Evaluate $\eta_1(t)$ either as a product of $t^{-q}/2$ and a truncated Taylor series of the term in parenthesis on the right-hand-side of Eq. (3.14) if t is sufficiently close to 0, or by direct subtraction otherwise.
3. Evaluate $\int_0^S K(t,s)\psi(s)|x(s)|^{-q}\,ds = \int_0^R K(t,s)\psi(s)|x(s)|^{-q}\,ds + \int_R^S K(t,s)\psi(s)|x(s)|^{-q}\,ds$. The first integral in the sum can be treated by a special one-sided Clenshaw–Curtis type quadrature described in Appendix A.2. In our experiments, we use between 31 points (for mild angles) and 255 points (for sharp angles). The second of these integrals can be efficiently and accurately approximated using classical Clenshaw–Curtis quadrature [46], with numbers of quadrature points varying between M and $2M$, for mild and sharp angles, respectively.
4. Evaluate $\int_S^T E_1(t,s)(T-s)^{-q}\,ds$ using a graded-mesh quadrature as described in Appendix A.1 using a number of quadrature points ranging between $M/2$ (for mild angles) and $2M$ (for sharp angles). We remark that, as t approaches 0, $E_1(t,s)$ generally builds up a (bounded) boundary-layer, as a function of s, near $s = T$—thus our selection of graded-mesh quadrature in this case, while Clenshaw–Curtis quadrature is perfectly adequate for $E_1(0,s)$.
5. Combine the results of steps 1–4 as indicated in Eq. (3.17).

For $t = 0$, our algorithm consists of the following steps:

1. Evaluate $\sigma_1(0) = \frac{V_1^{-q}\sin\alpha\pi}{2\pi q}$, the constant term of the series.
2. Evaluate $\eta_1(0) = 0$.
3. Evaluate $\int_0^S K(0,s)\psi(s)|x(s)|^{-q}\,ds$ as described above for $\int_0^S K(t,s)\psi(s)|x(s)|^{-q}\,ds$.
4. Evaluate $\int_S^T E_1(0,s)(T-s)^{-q}\,ds$ using a one-sided Clenshaw-Curtis type quadrature, using the same number of quadrature points as used above for $\int_0^R K(t,s)\psi(s)|x(s)|^{-q}\,ds$.
5. Combine the results of steps 1–4 as indicated in Eq. (3.17).

5 Need of special treatment of the leading singularity

Earlier in this text we indicated that the unbounded integral-equation solutions associated with the problems under consideration give rise to two main difficulties, namely,

Table 1 The integral $I(t_1)$ and approximate integral $\mathcal{I}(t_1)$ at the target point t_1 for the teardrop problem

p	M	t_1	$I(t_1)$	$\mathcal{I}(t_1)$
4	63	6.2×10^{-6}	2.4×10^{1}	2.8×10^{1}
4	127	3.8×10^{-7}	6.1×10^{1}	7.1×10^{1}
4	255	2.4×10^{-8}	1.6×10^{2}	1.8×10^{2}
4	511	1.5×10^{-9}	3.9×10^{2}	4.6×10^{2}
6	63	1.6×10^{-8}	1.8×10^{2}	2.4×10^{2}
6	127	2.4×10^{-10}	7.2×10^{2}	9.7×10^{2}
6	255	3.7×10^{-12}	2.9×10^{3}	3.9×10^{3}
6	511	5.7×10^{-14}	1.2×10^{4}	1.6×10^{4}
8	63	3.7×10^{-11}	1.3×10^{3}	2.1×10^{3}
8	127	1.4×10^{-13}	8.6×10^{3}	1.3×10^{4}
8	255	5.3×10^{-16}	5.5×10^{4}	8.5×10^{4}
8	511	2.1×10^{-18}	3.5×10^{5}	5.4×10^{5}
10	63	8.6×10^{-14}	1.0×10^{4}	1.8×10^{4}
10	127	8.0×10^{-17}	1.0×10^{5}	1.9×10^{5}
10	255	7.6×10^{-20}	1.1×10^{6}	1.9×10^{6}
10	511	7.3×10^{-23}	1.1×10^{7}	1.9×10^{7}

As the mesh is refined, t_1 approaches 0. The poor performance $\mathcal{I}(t_1)$ as an approximation of $I(t_1)$ shows that the quadrature (Eqs. A.1–A.4) cannot resolve the integral operator having $K(t, s)$ as its kernel for unbounded functions μ with singularities of the form [Eq. (3.1)]

occurrence of subtractive cancellations and reduced order of accuracy caused by the presence of unbounded integral-equation solutions. In this section we demonstrate, by means of a few simple examples, the extent to which these difficulties can affect numerical solutions unless a special treatment of the corner singularities such as that described in the previous sections is used. In detail, we demonstrate

1. The poor accuracy that results from use of graded-mesh Nyström integrators, unless recourse is made to some special interpolatory device [40] and significantly refined integration meshes; as well as,
2. The accuracy loss that occurs for t close to 0 and T unless the indeterminate limits that arise in the integral equations (2.21)–(2.22) as $t \to 0$ and $t \to T$ are adequately resolved.

Difficulty 1: Non-uniform integrability of the function $K(t, s)$. It is easy to verify by direct computation that $\int_0^T K(t, s)\, ds$ is unbounded as t approaches 0 or T, and the rate of blow-up is worsened for integrands $K(t, s)\mu(s)$ where $\mu(s)$ is unbounded near 0 and/or T. Graded-mesh quadratures such as those described in [2,22,36] provide very efficient integrators for integrands of the form $K(t, s)w(s)$ where w is the Hölder-continuous function that vanishes at the corner; such functions arises in integral methods for solutions of the *Dirichlet problem* provided adequate integral-equation formulations are used. As shown in Table 1, however, such quadratures are not sufficient by themselves to handle unbounded functions of the type we encounter in the Nyström formulation of the *Neumann problem*. In detail, since the quadrature points and target points in the Nyström method coincide, the integrator must, in particular, approximate accurately the integral

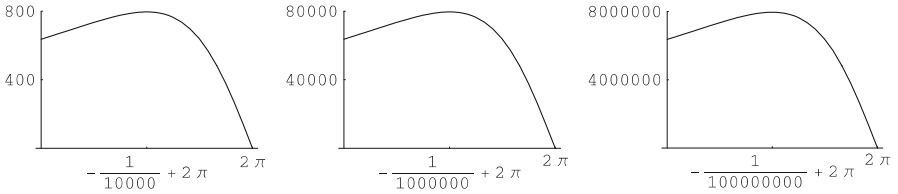

Fig. 2 Plots (in s) of the kernel $K(t,s)$ associated with the teardrop domain, having $\alpha = 1/2$, for $t = 10^{-4}, 10^{-6}, 10^{-8}$. Note the scales on the axes for the kernel plots

$$I(t_1) \equiv \int_0^T K(t_1,s)|x(s)|^{-q} \overset{?}{\approx} \mathcal{I}(t_1) \equiv \sum_{k=1}^{M} K(t_1,t_j)|x(t_j)|^{-q} w_j$$

at the mesh point t_1 that is closest to zero using the graded-mesh quadrature under consideration, which, in our case is defined by (A.1)–(A.4) with M points and power p.

To illustrate this difficulty we use a teardrop domain of the type depicted in Fig. 3 with $\alpha = 1/2$, $q = 1/3$. The kernel K shown Eq. (2.23) is depicted in Fig. 2 for various target points t near 0; these images display the general "diverging boundary-layer" behavior of the kernel around the corner. In Table 1, we present the target point t_1 nearest 0, the exact value of the integral $I(t_1)$, and the approximation $\mathcal{I}(t_1)$, for various values of M and p. We see that the quadrature significantly over-estimates the integral—never producing more than a single digit of accuracy!

Difficulty 2: Non-trivial subtractive cancellation at the corner. Even if the integral $K(t_1,s)|x(s)|^{-q}$ were computed accurately, a significant loss of accuracy may occur in the computation of the difference $f_1(t_1) = 0.5|x(t)|^{-q} - \int_0^T K(t_1,s)|x(s)|^{-q}\,ds$ due to subtractive cancellation—recall Remark 3.1. In Table 2, we demonstrate this issue by again considering the teardrop domain with $\alpha = 1/100$, $q = 99/199$. We report two relative errors:

$$\varepsilon_1(f_1(t_1)) = \left|\frac{f_1(t_1) - \tilde{f}_1(t_1)}{f_1(t_1)}\right| \quad \text{and} \quad \varepsilon_2(f_1(t_1)) = \left|\frac{f_1(t_1) - \bar{f}_1(t_1)}{f_1(t_1)}\right|.$$

Here, $\tilde{f}_1(t_1)$ is the value which we compute using the approach described in Eq. (3.17), and $\bar{f}_1(t_1)$ is the value that results from direct subtraction of 16-digit-accurate values of $0.5|x(t_1)|^{-q}$ and $\int_0^T K(t_1,s)|x(s)|^{-q}\,ds$. We see that our method of computing the difference, $\tilde{f}(t_1) \approx f(t_1)$, is very accurate and does not deteriorate as M and p are increased. The accuracy of the "direct-subtraction" method $\bar{f}(t_1) \approx f(t_1)$ deteriorates for fine discretizations as a result of massive subtractive cancellation.

6 Numerical results

In this section we demonstrate the performance of our algorithms for a variety of acute and obtuse interior angles $\alpha\pi$, including both mild and very sharp corner problems.

Table 2 Subtractive cancellation for the teardrop problem with $\alpha = 1/100$: relative errors in the approximation of $f_1(t_1)$ via our approach (3.17) (denoted by $\tilde{f}_1(t_1)$), and the direct approach (denoted by $\bar{f}_1(t_1)$), based on taking the difference in double precision of $|x(t_1)|^{-q}/2$ and $I(t_1)$—assuming that such 16-digit accurate values have been obtained

The loss of significance in $\bar{f}_1(t_1)$ due to subtractive cancellation becomes increasingly apparent as p and M increase

p	M	t_1	$\varepsilon_1(f_1(t_1))$	$\varepsilon_2(f_1(t_1))$
4	511	1.5×10^{-9}	6.6×10^{-11}	8.6×10^{-10}
4	1023	9.2×10^{-11}	4.2×10^{-12}	1.0×10^{-10}
4	2047	5.7×10^{-12}	2.8×10^{-13}	2.2×10^{-9}
4	4095	3.6×10^{-13}	4.7×10^{-14}	1.0×10^{-8}
6	511	5.7×10^{-14}	4.9×10^{-10}	1.0×10^{-7}
6	1023	8.8×10^{-16}	3.0×10^{-11}	1.7×10^{-7}
6	2047	1.4×10^{-17}	1.9×10^{-12}	7.4×10^{-6}
6	4095	2.1×10^{-19}	1.9×10^{-13}	9.3×10^{-6}
8	511	2.1×10^{-18}	3.3×10^{-13}	7.4×10^{-6}
8	1023	8.0×10^{-21}	7.4×10^{-14}	2.6×10^{-5}
8	2047	3.1×10^{-23}	5.4×10^{-14}	1.4×10^{-3}
8	4095	1.2×10^{-25}	4.8×10^{-14}	3.9×10^{-2}
10	511	7.3×10^{-23}	3.2×10^{-13}	3.8×10^{-4}
10	1023	7.0×10^{-26}	8.6×10^{-14}	3.9×10^{-2}
10	2047	6.9×10^{-29}	5.9×10^{-14}	1.2×10^{0}
10	4095	6.7×10^{-32}	5.8×10^{-14}	1.0×10^{0}

Table 3 Data for the teardrop problem, $\alpha = 1/2$, $q = 1/3$. Here, $\bar{x} = (1, 0)$ and $\hat{x} = (0.1, 0)$

p	N	$\varepsilon(a)$	$\varepsilon(\bar{u}^e)$	$\varepsilon(u^{iN}(\bar{x}))$	$\varepsilon(u^{iN}(\hat{x}))$	cond(A)
4	16	2.6×10^{-5}	2.2×10^{-6}	2.5×10^{-5}	3.7×10^{-8}	1.6×10^{1}
4	32	1.6×10^{-7}	3.6×10^{-8}	1.6×10^{-8}	3.5×10^{-8}	1.6×10^{1}
4	64	7.1×10^{-9}	1.5×10^{-11}	2.5×10^{-11}	5.9×10^{-11}	1.6×10^{1}
4	128	7.3×10^{-11}	1.0×10^{-11}	1.9×10^{-11}	3.0×10^{-12}	1.7×10^{1}
6	16	6.3×10^{-6}	1.4×10^{-5}	1.3×10^{-5}	2.0×10^{-6}	1.6×10^{1}
6	32	2.1×10^{-7}	1.1×10^{-7}	6.5×10^{-8}	8.4×10^{-8}	1.6×10^{1}
6	64	1.5×10^{-9}	1.4×10^{-11}	4.9×10^{-12}	2.6×10^{-10}	1.6×10^{1}
6	128	2.3×10^{-11}	5.9×10^{-12}	5.9×10^{-12}	1.7×10^{-12}	1.7×10^{1}
8	16	8.1×10^{-5}	3.8×10^{-5}	1.4×10^{-7}	1.6×10^{-6}	1.6×10^{1}
8	32	4.7×10^{-7}	1.8×10^{-7}	5.3×10^{-9}	3.0×10^{-8}	1.6×10^{1}
8	64	1.1×10^{-9}	4.9×10^{-12}	1.1×10^{-12}	4.2×10^{-10}	1.6×10^{1}
8	128	7.7×10^{-11}	8.0×10^{-12}	9.9×10^{-13}	1.7×10^{-13}	1.7×10^{1}

We have $a \approx 0.1904128401$ and $\bar{u}^e \approx -1.57770198749$

In Tables 1, 2, 3, 4, 5 and 6, we present algorithm parameters and resulting errors, including

- The power p in the graded-mesh quadrature (A.1)–(A.4) change-of-variables and the total number N of unknowns used in the discretization. For comparison with

Table 4 Data for the teardrop problem $\alpha = 1/100$, $q = 99/199$

$u^{iN}(x) = \ln\|x - \bar{z}\|$					$f(t) = (T - 3(\frac{t}{T})^2)/\|x'(t)\|$			
p	N	$\varepsilon(a)$	$\varepsilon(\bar{u}^e)$	$\varepsilon(u^{iN}(\bar{x}))$	p	N	$\varepsilon(a)$	$\varepsilon(\bar{u}^e)$
6	512	5.4×10^{-2}	9.5×10^{-4}	6.4×10^{-3}	6	512	1.3×10^{-1}	8.7×10^{-3}
6	1024	2.0×10^{-1}	4.9×10^{-3}	4.6×10^{-3}	6	1024	6.2×10^{-1}	1.5×10^{-1}
6	2048	2.3×10^{-4}	5.8×10^{-6}	5.4×10^{-6}	6	2048	6.7×10^{-4}	1.6×10^{-4}
6	4096	5.3×10^{-6}	5.0×10^{-7}	7.6×10^{-9}	6	4096	2.2×10^{-5}	5.3×10^{-6}
8	512	8.1×10^{-1}	6.7×10^{-2}	6.8×10^{-3}	8	512	1.1×10^{-0}	8.1×10^{-1}
8	1024	2.9×10^{-2}	7.3×10^{-4}	4.1×10^{-4}	8	1024	4.8×10^{-2}	1.7×10^{-2}
8	2048	2.8×10^{-4}	5.1×10^{-6}	6.3×10^{-6}	8	2048	8.3×10^{-4}	1.4×10^{-4}
8	4096	2.1×10^{-6}	1.9×10^{-7}	2.8×10^{-9}	8	4096	4.2×10^{-6}	2.0×10^{-6}
10	512	1.7×10^{-1}	1.9×10^{-2}	5.6×10^{-3}	10	512	2.8×10^{-2}	1.3×10^{-1}
10	1024	9.9×10^{-3}	5.4×10^{-4}	3.4×10^{-4}	10	1024	3.0×10^{-2}	1.6×10^{-2}
10	2048	3.1×10^{-4}	1.1×10^{-5}	3.6×10^{-6}	10	2048	8.9×10^{-4}	2.9×10^{-4}
10	4096	9.3×10^{-7}	1.2×10^{-8}	7.0×10^{-10}	10	4096	2.8×10^{-6}	3.1×10^{-7}

Here, $\bar{x} = (0.1, 0)$. In the first case, $a \approx 0.1310937$ and $\bar{u}^e \approx -1.5982659$. In the second case, $a \approx -18.92685$ and $\bar{u}^e \approx -24.206462$

Table 5 Data for the boomerang-shaped domain, $\alpha = 3/2$, $q = 1/3$

$u^{iN}(x) = \ln\|x - \bar{z}\|$				$u^{iN}(x) = \alpha r^{1/\alpha} \sin(\theta/\alpha)$			
p	N	$\|a\|$	$\varepsilon(u^{iN}(\bar{x}))$	p	N	$\varepsilon(a)$	$\varepsilon(u^{iN}(\bar{x}))$
6	32	5.6×10^{-17}	5.7×10^{-8}	6	32	6.4×10^{-5}	5.4×10^{-5}
6	64	5.5×10^{-18}	4.7×10^{-11}	6	64	3.6×10^{-7}	2.4×10^{-7}
6	128	1.4×10^{-17}	5.0×10^{-15}	6	128	4.2×10^{-10}	4.4×10^{-10}
6	256	6.8×10^{-17}	1.3×10^{-16}	6	256	4.2×10^{-11}	2.9×10^{-12}

Here $\bar{x} = (0.1, 0.1)$. In the former case, $a = 0$, and in the latter, $a = \sqrt{3}$

Table 6 Data for the heart-shaped domain, $\alpha = 199/100$, $q = 99/199$

$u^{iN}(x) = \ln\|x - \bar{z}\|$				$f(t) = (T - 3(\frac{t}{T})^2)/\|x'(t)\|$			
p	N	$\|a\|$	$\varepsilon(u^{iN}(\bar{x}))$	p	N	$\varepsilon(a)$	$\varepsilon(\bar{u}^e)$
6	32	2.6×10^{-9}	4.3×10^{-7}	8	512	7.4×10^{-1}	7.4×10^{-1}
6	64	2.1×10^{-9}	7.4×10^{-9}	8	1024	4.1×10^{-2}	4.1×10^{-2}
6	128	1.9×10^{-12}	2.7×10^{-11}	8	2048	1.9×10^{-2}	1.9×10^{-2}
6	256	3.2×10^{-16}	1.0×10^{-14}	8	4096	1.1×10^{-4}	1.1×10^{-4}

Here $\bar{x} = (0.1, 0.1)$. In the former case, $a = 0$. In the latter case, $a \approx -88.896$ and $\bar{u}^e \approx -178.076$

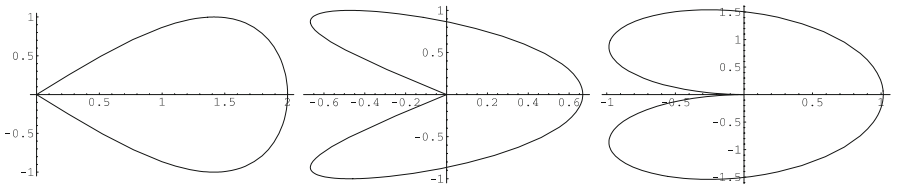

Fig. 3 The teardrop domain (*left*) with $\alpha = 1/2$, the boomerang-shaped domain with $\alpha = 3/2$, and the heart-shaped domain with $\alpha = 199/100$

the results in [36] for Dirichlet problems, note that the n reported in the tables given there corresponds to $N/2$ in our case.

- The relative error $\varepsilon(a) = |(a - \tilde{a})/a|$ in our approximation $\tilde{a} \approx a$. When a is not known explicitly (as is most often the case), we use our computed value for the largest reported p and twice our largest reported N as the "exact" value. When $a = 0$, we report $|a|$ instead.
- The relative error $\varepsilon(\bar{u}^e) = |(\bar{u}^e - \tilde{u}^e)/\bar{u}^e|$ in our approximation $\tilde{u}^e \approx \bar{u}^e$. We use our computed value for the largest reported p and twice our largest reported N as the "exact" value.
- The relative error $\varepsilon(u^{iN}(x)) = |(u^{iN}(x) - \tilde{u}^{iN}(x))/u^{iN}(x)|$ in our approximation $\tilde{u}^{iN}(x) \approx u^{iN}(x)$ at one or two interior points, when the exact solution $u^{iN}(x)$ is known. The approximate solution is computed by means of Eq. (2.5) using appropriate quadratures and our numerical solutions a, $\bar{u}^e$ and μ_2.
- An estimate cond(A) of the condition number of the system matrix. We only provide this quantity in cases in which a reliable estimate of it could easily be produced—which occurred for corners that are not too sharp.

Acute interior angles—teardrop domains. For acute interior angles, we concentrate on a family of domains bounded by the curves

$$x(t) = \left(2 \sin \frac{t}{2},\ -\beta \sin t\right), \quad \beta = \tan \frac{\alpha\pi}{2}, \quad 0 < \alpha < 1, \quad 0 \le t \le 2\pi, \qquad (6.1)$$

see Fig. 3. We consider the mild case $\alpha = 1/2$, and the extreme case $\alpha = 1/100$ for which the domain is essentially a needle.

For our first set of teardrop experiments, for $\alpha = 1/2$, we choose boundary data corresponding to the exact solution $u^{iN}(x) = \ln|x - \bar{z}|$, with $\bar{z} = (6, 0) \in \mathbb{R}^2 \backslash \overline{\Omega}$. The data is reported in Table 3. The overall performance of the method is excellent, resulting in at least 10-digit accuracies using a small number of discretization points—significantly more accurate than any other previous solver for such mild corner problems.

Our next example demonstrates the performance of our approach on the rather extreme case $\alpha = 1/100$, for which the domain is essentially a needle. In Table 4 we present results for two $\alpha = 1/100$ experiments: one for which the exact solution is known and equals $u^{iN}(x) = \ln|x - \bar{z}|$, and the other one with Neumann conditions given by the zero-average ($\int_0^T f(t)|x'(t)|\,dt = 0$) function $f(t) = (T - 3(\frac{t}{T})^2)/|x'(t)|$—for which the exact solution is not available. As expected, the present $\alpha = 1/100$-problem is much more challenging than the $\alpha = 1/2$-problem

considered previously; yet our method still produces up to 7 digits of accuracy in the PDE solution and other observables. We conjecture that, by incorporating additional terms in our special treatment of the asymptotic series, and perhaps modifying the linear system adequately, it may be possible to achieve a performance similar to that obtained for $\alpha = 1/2$, even for extreme angles; this topic lies beyond the scope of the present contribution, and is left for future work.

Obtuse interior angles—boomerang-shaped and heart-shaped domains. Here we consider two families of domains: boomerang-shaped [36] and heart-shaped domains. Letting $\beta = \tan\frac{\alpha\pi}{2}$, we define the former domains as those bounded by the curves

$$x(t) = \left(-\frac{2}{3}\sin\frac{3t}{2},\ \beta\sin t\right), \quad 1 < \alpha < 2, \quad 0 \le t \le 2\pi; \tag{6.2}$$

the heart-shaped domains, in turn, are those bounded by the curves

$$x(t) = \begin{pmatrix}\cos(1+\alpha)t & -\sin(1+\alpha)t\\ \sin(1+\alpha)t & \cos(1+\alpha)t\end{pmatrix}\begin{pmatrix}\beta\\ 1\end{pmatrix} - \begin{pmatrix}\beta\\ \cos t\end{pmatrix}, \quad 1 < \alpha < 2, \quad 0 \le t \le \pi. \tag{6.3}$$

Samples of boomerang-shaped and heart-shaped domains are presented in Fig. 3. The reason for including the heart-shaped domain in addition to the previously considered [36] boomerang-shaped domains is that, for α near 2, the parameterization of the boomerang-shaped domain has derivatives which vary widely, with speeds $|x'(t)|$ that are very small at some points. This negatively affects the behavior of the kernel, the conditioning of the system, and the performance of the algorithm. Rather than reparameterize these curves, we opted to include the heart-shaped domains, for which the corner angle is just as easy to control and which do not suffer from this difficulty.

In Table 5, we present results for two problems involving the boomerang-shaped domain, with $\alpha = 3/2$, with respective Neumann boundary data corresponding to two known solutions: $u^{iN}(x) = \ln|x - \bar{z}|$, $\bar{z} = (6, 0)$, and $u^{iN}(x) = \alpha r^{1/\alpha}\sin(\theta/\alpha)$; we note that the Dirichlet version of the second problem is considered in [36]. The first choice illustrates that the expected blow up of the integral-equation solution for obtuse corner angles may not occur. Here we have $a = 0$, as is easy to check by specializing the analysis of Sect. 2 to the present context: in this case u^{iN} does not contain an $r^{1/\alpha}$-type singularity near the origin (it is analytic in a neighborhood of the origin), so the complementary u^{eD} cannot inherit such a singularity through the boundary conditions. Therefore, the leading singular exponent for u^{eD} is $1/(2-\alpha) - 1 > 0$, and the density does not blow up near the corner. The second choice, $u^{iN}(x) = \alpha r^{1/\alpha}\sin(\theta/\alpha)$, gives us an example in which we can compute the coefficient a analytically. Once again, following the analysis of Sect. 2 we obtain $u^{eD} \sim -\alpha\sec\left(\frac{\pi}{\alpha}\right) r^{1/\alpha}\sin\left(\frac{\theta-\pi}{\alpha}\right)$ as $r \to 0$, and hence that $\phi \sim \pm\tan\left(\frac{\pi}{\alpha}\right) r^{1/\alpha-1}$ as $r \to 0$ along Γ. The "+" and "−" signs corresponds to the limits as $r \to 0$ along Γ in the lower and upper half-planes, respectively. We therefore find that $\mu(t) = -\tan\left(\frac{\pi}{\alpha}\right)\mu_1(t) + \mu_2(t) = \sqrt{3}\mu_1(t) + \mu_2(t)$. Our algorithm displays excellent performance for both problems

considered in Table 5—in the second case this it true in spite of the fact that the Neumann data is not even of class C^1 on either Γ_1 or Γ_2. The condition numbers of the associated matrices are quite mild: they range between about 10 and 25 for these experiments.

In Table 6, we display results produced by our algorithm for the heart-shaped domain with $\alpha = 199/100$. This is a obtuse-angle counterpart of the $\alpha = 1/100$ teardrop problem, and, as before, we use boundary data given by the normal derivative of the function $u^{iN}(x) = \ln|x - \bar{z}|$. The performance is once again very good indeed, note that, as in a previous case, here we have $a = 0$. For the more generic Neumann data $f(t) = (T - 3(\frac{t}{T})^2)/|x'(t)|$ the problem is much more difficult, as it was for the $\alpha = 1/100$-teardrop; in this case our method produces four digits of accuracy. Curiously, the relative errors for a and $\bar{u}^e$ reported in Table 6, though not identical, do agree with each other to the precision shown. As suggested above in connection with the case involving a sharp needle, here we conjecture that, by incorporating additional terms in our special treatment of the asymptotic series, and perhaps modifying the linear system adequately, it may be possible to achieve, in the sharp-angle case, a performance similar to that obtained for mild angles.

Appendix A: Quadratures and kernel evaluation

In this appendix we collect details concerning the implementation of our algorithm.

A.1 Graded-mesh quadratures

We present a simple global quadrature rule for all the integrals involving the Hölder-continuous function μ_2, namely

$$\int_0^T K(t,s)\mu_2(s)\,ds, \quad \int_0^T \mu_2(s)|x'(s)|\,ds \quad \text{and} \quad \int_0^T \mu_2(s)|x'(s)|\ln|x(s)|\,ds.$$

The algorithm provided for the first of these integration problems should be uniformly accurate regardless of the proximity of the target point t to $t = 0$ or $t = T$. The latter two integration problems are related to the zero-mean condition $\int_0^T \mu(s)|x'(s)|\,ds = 0$ and the computation of the constant $\bar{u}^e$, respectively—taking $x_0 = 0$ for the computation of $\bar{u}^e$ in Eq. (2.5). We briefly describe the approach introduced and analyzed in [36].

To approximate integrals of the type $I = \int_a^b g(s)\,ds$, we use the change-of-variables

$$v(x) = (b-a)\frac{[c(x)]^p}{[c(x)]^p + [1-c(x)]^p} + a \tag{A.1}$$

for an integer $p \geq 2$, where

$$c(x) = \left(\tfrac{1}{2} - \tfrac{1}{p}\right)\left(\tfrac{2x-b-a}{b-a}\right)^3 + \tfrac{1}{p}\left(\tfrac{2x-b-a}{b-a}\right) + \tfrac{1}{2}. \tag{A.2}$$

The bijection $v : [a, b] \to [a, b]$ is analytic, and it has $p - 1$ vanishing derivatives at a and b.

With this change-of-variables, we have

$$I = \int_a^b g(t)\,dt = \int_a^b g(v(s))v'(s)\,ds \approx \sum_{k=1}^{N} w_k g(t_k), \tag{A.3}$$

where the approximate expression was obtained by using the trapezoid rule on the integral including the change-of-variables, and where

$$x_k = \frac{k(b-a)}{N+1}, \quad t_k = v(x_k) \quad \text{and} \quad w_k = \tfrac{b-a}{N+1}\, v'(x_k), \quad 1 \leq k \leq N. \tag{A.4}$$

A.2 Clenshaw–Curtis quadratures

Here we describe efficient and accurate quadrature rules for integrals of the forms

$$\int_0^S K(t,s)\psi(s)|x(s)|^{-q}\,ds \quad \text{for } t \in [0, \hat{S}], \qquad \int_0^T \psi(s)|x(s)|^{-q}|x'(s)|\,ds, \tag{A.5}$$

$$\int_R^T K(t,s)\psi(s)|x(s)|^{-q}\,ds \quad \text{for } t \in [\hat{R}, T], \qquad \int_0^T \psi(s)|x(s)|^{-q}|x'(s)|\ln|x(s)|\,ds. \tag{A.6}$$

The integrand in each of these integrals is given by the product of a smooth function and a function that contains a known singularity at either one or both of its endpoints, and is otherwise smooth. We derive appropriate Clenshaw–Curtis-type quadratures for these problems: such quadrature rules have a practical advantage over their Gaussian quadrature counterparts, since their quadrature points and weights are fairly simple and inexpensive to compute, and yet they display outstanding performance [30,42,46,47].

A.2.1 One-sided power and logarithmic singularities

Without loss of generality, we can take the singularities to lie at the left endpoint. Clearly, further, it suffices to produce quadrature rules for integrals of the forms

$$I_1 = \int_a^b g(t)(t-a)^{-\kappa}\,dt, \quad I_2 = \int_a^b g(t)(t-a)^{-\kappa}\ln(t-a)\,dt,$$

where $\kappa < 1$ and g is a Hölder continuous on (a, b) with positive Hölder exponent, since the integrals containing the kernel $K(t, s)$ in Eqs. (A.5) and (A.6) can be re-expressed in the form

$$\int_0^S K(t,s)\psi(s)\left|\frac{x(s)}{s}\right|^{-q} s^{-q}\,ds \quad \text{and} \quad \int_0^{T-R} K(t,T-u)\psi(T-u)\left|\frac{x(T-u)}{u}\right|^{-q} u^{-q}\,ds.$$

Integrals of the I_2-sort naturally arise in computations which, like those in Eq. (2.5), involve the single-layer potential.

To obtain the desired quadrature rules we begin by transforming the integrals to the forms

$$\begin{aligned} I_1 &= (b-a)^{1-\kappa}2^{\kappa-1}\int_{-1}^{1}\hat{g}(x)\,(1+x)^{-\kappa}\,dx \\ I_2 &= (b-a)^{1-\kappa}2^{\kappa-1}\int_{-1}^{1}\hat{g}(x)\,(1+x)^{-\kappa}\left(\ln(b-a)+\ln\left(\frac{1+x}{2}\right)\right)dx \\ &= \ln(b-a)I_1 + (b-a)^{1-\kappa}2^{\kappa-1}\int_{-1}^{1}\hat{g}(x)\,(1+x)^{-\kappa}\ln\left(\frac{1+x}{2}\right)dx, \end{aligned}$$

where $\hat{g}(x) = g\left(\frac{b-a}{2}x + \frac{b+a}{2}\right)$. We have thus reduced the problem to evaluating the integrals

$$\hat{I}_1 = 2^{\kappa-1}\int_{-1}^{1}\hat{g}(x)\,(1+x)^{-\kappa}\,dx \quad \text{and} \quad \hat{I}_2 = 2^{\kappa-1}\int_{-1}^{1}\hat{g}(x)\,(1+x)^{-\kappa}\ln\left(\frac{1+x}{2}\right)dx,$$

where we have kept the factor $2^{\kappa-1}$ for convenience in later recurrence relations.

The Chebyshev series of $\hat{g}(x)$ is

$$\hat{g}(x) = {\sum_{n=0}^{\infty}}' c_n T_n(x) \quad \text{for} \quad c_n = \frac{2}{\pi}\int_{-1}^{1}\frac{\hat{g}(x)T_n(x)}{\sqrt{1-x^2}}\,dx = \frac{2}{\pi}\int_0^{\pi}\hat{g}(\cos\theta)\,\cos n\theta\,d\theta,$$

with the convention that the prime in the sum indicates that the 0th term is halved. We obtain the series expansions

$$\hat{I}_1 = \sum_{n=0}^{\infty}{}' c_n \alpha_n \quad \alpha_n = 2^{\kappa-1} \int_{-1}^{1} T_n(x)\,(1+x)^{-\kappa}\,dx$$

$$\hat{I}_2 = \sum_{n=0}^{\infty}{}' c_n \beta_n \quad \beta_n = 2^{\kappa-1} \int_{-1}^{1} T_n(x)\,(1+x)^{-\kappa} \ln\left(\frac{1+x}{2}\right) dx$$

which, in our numerical method, we truncate to $M+1$ terms. The coefficients c_n are computed, of course, using a Type-I Discrete Cosine Transform entailing a $\mathcal{O}(M \log M)$ cost. The coefficients α_n and β_n, in turn, are evaluated analytically in an efficient manner by means of the recursive relations given in Lemma A.1 below. Thus, the quadrature rules under consideration are defined by

$$\hat{I}_1 \approx \sum_{n=0}^{M}{}' \tilde{c}_n \alpha_n = \sum_{k=0}^{M}{}'' w_k^{\alpha} g(t_k) \qquad \hat{I}_2 \approx \sum_{n=0}^{M}{}' \tilde{c}_n \beta_n = \sum_{k=0}^{M}{}'' w_k^{\beta} g(t_k),$$

where the double prime on the sum indicates that both the 0^{th} and M^{th} terms are halved, $t_k = \frac{b-a}{2} \cos\frac{k\pi}{M} + \frac{b+a}{2}$ and

$$w_k^{\alpha} = \sum_{n=0}^{M}{}' \frac{2\alpha_n}{M} \cos\frac{nk\pi}{M} \qquad w_k^{\beta} = \sum_{n=0}^{M}{}' \frac{2\beta_n}{M} \cos\frac{nk\pi}{M}.$$

Consequently, all that remains is for us to devise an efficient means for evaluation of the coefficients α_n, β_n. We do so via simple recurrence relations, and use two key recurrences for T_n in the derivation:

1. $T_0(x) = 1$, $T_1(x) = x$, and $T_{n+1}(x) = 2xT_n(x) - T_{n-1}(x)$ for $n \geq 1$
2. $2T_n(x) = \dfrac{d}{dx}\left(\dfrac{T_{n+1}(x)}{n+1} - \dfrac{T_{n-1}(x)}{n-1}\right)$ for $n > 1$

Direct computation yields that the first few values of α_n and β_n are:

$$\alpha_0 = \frac{1}{1-\kappa}, \quad \alpha_1 = \frac{2}{2-\kappa} - \frac{1}{1-\kappa}, \quad \alpha_2 = \frac{8}{3-\kappa} - \frac{8}{2-\kappa} + \frac{1}{1-\kappa}$$
$$\beta_0 = -\frac{1}{(1-\kappa)^2}, \quad \beta_1 = -\frac{2}{(2-\kappa)^2} + \frac{1}{(1-\kappa)^2},$$
$$\beta_2 = -\frac{8}{(3-\kappa)^2} + \frac{8}{(2-\kappa)^2} - \frac{1}{(1-\kappa)^2}.$$

Using these values and the following lemma, all coefficients α_n and β_n can be obtained.

Lemma A.1 *For $n > 1$ we have the recurrences*

$$\alpha_{n+1} = -\frac{n+1}{n-\kappa+2}\left(\frac{2}{n^2-1} + 2\alpha_n + \frac{n+\kappa-2}{n-1}\,\alpha_{n-1}\right)$$
$$\beta_{n+1} = -\frac{n+1}{n-\kappa+2}\left(\frac{\alpha_{n+1}}{n+1} - \frac{\alpha_{n-1}}{n-1} + 2\beta_n + \frac{n+\kappa-2}{n-1}\,\beta_{n-1}\right).$$

Proof For $n > 1$, we have

$$\begin{aligned}
\alpha_{n+1} &= 2^{\kappa-1}\int_{-1}^{1} 2T_n(x)(1+x)^{1-\kappa}\,dx - 2\alpha_n - \alpha_{n-1} \\
&= 2^{\kappa-1}\int_{-1}^{1} \frac{d}{dx}\left(\frac{T_{n+1}(x)}{n+1} - \frac{T_{n-1}(x)}{n-1}\right)(1+x)^{1-\kappa}\,dx - 2\alpha_n - \alpha_{n-1} \\
&= -\frac{2}{n^2-1} - 2\alpha_n - \alpha_{n-1} - 2^{\kappa-1}\int_{-1}^{1}\left(\frac{T_{n+1}(x)}{n+1} - \frac{T_{n-1}(x)}{n-1}\right)\frac{d}{dx}(1+x)^{1-\kappa}\,dx \\
&= -\frac{2}{n^2-1} - 2\alpha_n - \alpha_{n-1} - \frac{1-\kappa}{n+1}\,\alpha_{n+1} + \frac{1-\kappa}{n-1}\,\alpha_{n-1} \\
&= -\frac{n+1}{n-\kappa+2}\left(\frac{2}{n^2-1} + 2\alpha_n + \frac{n+\kappa-2}{n-1}\,\alpha_{n-1}\right).
\end{aligned}$$

The assumption $n > 1$ is needed for the second equality. The same kind of argument yields the recurrence for β_{n+1}.

A.2.2 Two-sided power and logarithmic singularities

In this subsection, we devise quadrature rules for integrals of the forms

$$\begin{aligned}
I_1 &= \int_a^b g(t)[(t-a)(b-t)]^{-\kappa}\,dt \quad \text{and} \\
I_2 &= \int_a^b g(t)[(t-a)(b-t)]^{-\kappa}\ln[(t-a)(b-t)]\,dt,
\end{aligned} \tag{A.7}$$

where $\kappa < 1$ and g is a Hölder-continuous on (a, b) with positive Hölder-exponent. The integral

$$\int_0^T \psi(s)|x'(s)| \left|\frac{x(s)}{s(s-T)}\right|^{-q} [s(T-s)]^{-q} \left(\ln\left|\frac{x(s)}{s(s-T)}\right| + \ln(s(T-s))\right) ds,$$

arising in the computation of the single-layer integrals in (2.5), motivates our development of quadrature rules for integrals of the types (A.7). As before, using changes of variables we obtain

$$I_1 = (b-a)^{1-2\kappa}\, 2^{2\kappa-1} \int_{-1}^{1} \hat{g}(x)\,(1-x^2)^{-\kappa}\, dx$$

$$I_2 = (b-a)^{1-2\kappa}\, 2^{2\kappa-1} \int_{-1}^{1} \hat{g}(x)\,(1-x^2)^{-\kappa} \left(2\ln\left(\frac{b-a}{2}\right) + \ln(1-x^2)\right) dx$$

$$= 2\ln\left(\frac{b-a}{2}\right) I_1 + (b-a)^{1-2\kappa}\, 2^{2\kappa-1} \int_{-1}^{1} \hat{g}(x)\,(1-x^2)^{-\kappa} \ln(1-x^2)\, dx.$$

The problem has thus been reduced to that of finding quadratures for

$$\hat{I}_1 = 2^{2\kappa-1} \int_{-1}^{1} \hat{g}(x)\,(1-x^2)^{-\kappa}\, dx \quad \hat{I}_2 = 2^{2\kappa-1} \int_{-1}^{1} \hat{g}(x)\,(1-x^2)^{-\kappa} \ln(1-x^2)\, dx,$$

which is further reduced to computing the quantities:

$$\alpha_n = 2^{2\kappa-1} \int_{-1}^{1} T_n(x)(1-x^2)^{-\kappa}\, dx \quad \beta_n = 2^{2\kappa-1} \int_{-1}^{1} T_n(x)(1-x^2)^{-\kappa} \ln(1-x^2)\, dx.$$

It is clear from the parity of the integrands that $\alpha_n = \beta_n = 0$ when n is odd. Quadrature rules for the integrals $\hat{I}_1$, were the scope of investigation in [30], although the approach therein is slightly different than the method that we present in what follows.

Direct calculations yield the initial values of α_n and β_n:

$$\alpha_0 = \frac{\Gamma^2(1-\kappa)}{\Gamma(2-2\kappa)} \qquad \beta_0 = \frac{\Gamma^2(1-\kappa)}{\Gamma(2-2\kappa)}(\psi_0(1-\kappa) - \psi_0(1.5-\kappa)),$$

where $\Gamma(x)$ is the gamma-function and $\psi_0(x) = \Gamma'(x)/\Gamma(x)$ is the digamma-function. In the special case $\kappa = 0.5$, the coefficients α_n and β_n can be seen to equal

$\alpha_0 = \pi$, $\beta_0 = -2\pi \ln 2$ and $\alpha_n = \beta_n = 0$ for $n \geq 1$. The recurrences result from similar arguments to those followed for the one-sided singularity problem; the resulting recursions are presented in the following lemma.

Lemma A.2 *For $n \geq 1$ we have the recurrences*

$$\alpha_{n+1} = \frac{n + 2\kappa - 2}{n - 2\kappa + 2}\,\alpha_{n-1} \qquad \beta_{n+1} = \frac{n + 2\kappa - 2}{n - 2\kappa + 2}\,\beta_{n-1} - \frac{4n}{(n - 2\kappa + 2)^2}\,\alpha_{n-1}.$$

Or, expressed in terms of even and odd subscripts

$$\alpha_{2n} = \frac{2n + 2\kappa - 3}{2n - 2\kappa + 1}\,\alpha_{2n-2} \qquad \alpha_{2n-1} = 0,$$

$$\beta_{2n} = \frac{2n + 2\kappa - 3}{2n - 2\kappa + 1}\,\beta_{2n-2} - \frac{8n - 4}{(2n - 2\kappa + 1)^2}\,\alpha_{2n-2} \qquad \beta_{2n-1} = 0.$$

A.3. Evaluation of K, E_1 and E_2

To achieve the accuracies reported in Sect. 6, it is necessary to use some care in the evaluation of the integral kernels K, E_1 and E_2. In this subsection we discuss and address the key issues in these regards.

Recalling that the kernel $K(t, s)$ contains the difference $x(t) - x(s)$ in both its numerator and denominator, we seek to avoid unnecessary loss of significance in the evaluation of $K(t, s)$ due to subtractive cancellation in $x(t) - x(s)$ when s is near t—as is often the case in our solvers, owing to our use of graded meshes. We do this by means of polynomial interpolation with equispaced knots taken from the set

$$\{\cdots, t - 2\delta, t - \delta, t, t + \delta, t + 2\delta, \cdots\},$$

where the stepsize δ is appropriately small, but not so small that it gives rise subtractive cancellation. In our computations we use an odd number of knots which always includes the point t, and we center the knots around t when possible—otherwise we get as close as we can to having t be the central knot. We evaluate $K(t, s)$ directly when s is sufficiently far from t, and via the polynomial interpolant otherwise. Because $K(t, s)$ is smooth for s near t, this polynomial approximation is highly accurate.

This type of cancellation problem does not occur in connection with either of the kernels E_1 and E_2, since these kernels arise in situations where s and t are far from each other only, but describe points which are spatially close to each other, but on opposite sides of the corner. In these cases, we opt for approximations which are constructed on the basis of Taylor series expansions. Because the approaches we use to eliminate cancellation errors for E_1 and E_2 are analogous, we only describe the one we use for E_1. Recalling that $E_1(t, s) = L_1(t, s)|x'(T)|^{-q} - K(t, s)|x(s)/(s - T)|^{-q}$, we note that, as the target point t approaches 0 and the integration point s approaches T, both terms $L_1(t, s)$ and $K(t, s)$ are unbounded, yet their difference is finite, so we must again design an algorithm to avoid potentially substantial subtractive cancellation.

To this end, we begin by decomposing E_1 into three terms, $E_1(t,s) = E_{11}(t,s) + E_{12}(t,s) + E_{13}(t,s)$ defined as

$$E_{11}(t,s) = -\frac{x(t)\cdot n(t)}{2\pi|x(t)-x(s)|^2}\,|x'(s)|\left|\frac{x(s)}{s-T}\right|^{-q}$$

$$E_{12}(t,s) = \frac{x(s)\cdot n(t)\,|x'(s)|\left|\frac{x(s)}{s-T}\right|^{-q} - (s-T)x'(T)\cdot n(0)\,|x'(T)|^{1-q}}{2\pi|tx'(0)-(s-T)x'(T)|^2}$$

$$E_{13}(t,s) = \frac{|tx'(0)-(s-T)x'(T)|^2 - |x(t)-x(s)|^2}{2\pi|x(t)-x(s)|^2|tx'(0)-(s-T)x'(T)|^2}\,x(s)\cdot n(t)\,|x'(s)|\left|\frac{x(s)}{s-T}\right|^{-q}.$$

In each of these terms, we must handle the subtractive cancellation in the numerators of each fraction when t and s are near their respective endpoints; in the first of these denominators the subtractive cancellation occurs in the inner product $x(t)\cdot n(t)$. We eliminate all of these subtractive cancellations, quite simply, by means of Taylor approximations centered at $t = 0$ and/or $s = T$. In our implementation we truncate the series at the point beyond which it would be necessary to evaluate more than three derivatives of the position or normal vectors x, n at $0, T$ to continue the expansion. Finally, we mention the special case,

$$E_1(0,s) = \frac{1}{2\pi(s-T)}\left(\frac{x(s)}{s-T}\cdot n(0)\,|x'(s)|\left|\frac{x(s)}{s-T}\right|^{-(2+q)} - |x'(T)|^{-q}\,\sin\alpha\pi\right),$$

which we evaluate directly when s is far enough from T, and otherwise via a Taylor series expansion, as indicated above.

References

1. Atkinson KE (1997) The numerical solution of integral equations of the second kind. Cambridge monographs on applied and computational mathematics , vol 4. Cambridge University Press, Cambridge
2. Atkinson KE, Graham IG (1988) An iterative variant of the Nyström method for boundary integral equations on nonsmooth boundaries. The mathematics of finite elements and applications, VI (Uxbridge, 1987), London, pp 297–303
3. Babuška I, Kellogg RB, Pitkäranta J (1979) Direct and inverse error estimates for finite elements with mesh refinements. Numer Math 33:447–471
4. Babuška I, von Petersdorff T, Andersson B (1994) Numerical treatment of vertex singularities and intensity factors for mixed boundary value problems for the Laplace equation in $\mathbf{R}^3$. SIAM J Numer Anal 31:1265–1288
5. Babuška I, Miller A (1984) The post-processing approach in the finite-element method, 2: The calculation of stress intensity factors. Int J Numer Methods Eng 20:1111–1129
6. Björck Å (1996) Numerical methods for least squares problems. Society for Industrial and Applied Mathematics (SIAM), Philadelphia
7. Bleszynski E, Bleszynski M, Jaroszewicz T (1996) AIM: adaptive integral method for solving large-scale electromagnetic scattering and radiation problems. Radio Sci 31:1225–1251
8. Borsuk M, Kondrat′ev V (2006) Elliptic boundary value problems of second order in piecewise smooth domains, vol 69. North-Holland Mathematical Library. Elsevier, Amsterdam (2006)
9. Bruno OP, Kunyansky LA (2001) A fast, high-order algorithm for the solution of surface scattering problems: basic implementation, tests, and applications. J Comput Phys 169:80–110

10. Costabel M, Ervin VJ, Stephan EP (1993) Quadrature and collocation methods for the double layer potential on polygons. Z Anal Anwendungen 12:699–707
11. Costabel M, Stephan E (1983) Curvature terms in the asymptotic expansions for solutions of boundary integral equations on curved polygons. J Integr Equ 5:353–371
12. Costabel M, Stephan E (1983) The normal derivative of the double layer potential on polygons and Galerkin approximation. Appl Anal 16:205–228
13. Costabel M, Stephan E (1985) Boundary integral equations for mixed boundary value problems in polygonal domains and Galerkin approximation. Mathematical models and methods in mechanics, Banach Center Publ. 15, Warsaw, pp 175–251
14. Costabel M, Dauge M (2000) Singularities of electromagnetic fields in polyhedral domains. Arch Ration Mech Anal 151:221–276
15. Cox C, Fix G (1985) On the accuracy of least squares methods in the presence of corner singularities. Comput Math Appl 10:463–475
16. Demkowicz L, Devloo P, Oden J (1985) On an h-type mesh-refinement strategy based on minimization of interpolation errors. Comput Methods Appl Mech Eng 53:67–89
17. Devloo P (1990) Recursive elements, an inexpensive solution process for resolving point singularities in elliptic problems. In: Proceedings of 2nd World Congress on Computational Mechanics. IACM, Stuttgart, pp 609–612
18. Elschner J, Jeon Y, Sloan IH, Stephan EP (1997) The collocation method for mixed boundary value problems on domains with curved polygonal boundaries. Numer Math 76:355–381
19. Elschner J, Stephan EP (1996) A discrete collocation method for Symm's integral equation on curves with corners. J Comput Appl Math 75:131–146
20. Fix GJ, Gulati S, Wakoff GI (1973) On the use of singular functions with finite element approximations. J Comput Phys 13:209–228
21. Ganesh M, Graham IG (2004) A high-order algorithm for obstacle scattering in three dimensions. J Comput Phys 198:211–242
22. Graham IG, Chandler GA (1988) High-order methods for linear functionals of solutions of second kind integral equations. SIAM J Numer Anal 25:1118–1137
23. Grisvard P (1985) Elliptic problems in nonsmooth domains. Monographs and Studies in Mathematics, vol 24. Pitman (Advanced Publishing Program), Boston
24. Grisvard P (1992) Singularities in boundary value problems. Recherches en Mathématiques Appliquées (Research in Applied Mathematics), vol 22. Masson, Paris
25. Givoli D, Rivkin L, Keller JB (1992) A finite element method for domains with corners. Int J Numer Methods Eng 35:1329–1345
26. Heuer N, Mellado ME, Stephan EP (2002) A p-adaptive algorithm for the BEM with the hypersingular operator on the plane screen. Int J Numer Methods Eng 53:85–104
27. Heuer N, Stephan EP (1996) The hp-version of the boundary element method on polygons. J Int Equations Appl 8:173–212
28. Heuer N, Stephan EP (1998) Boundary integral operators in countably normed spaces. Math Nachr 191:123–151
29. Hughes T, Akin J (1980) Techniques for developing 'special' finite element shape function with particular reference to singularities. Int J Numer Methods Eng 15:733–751
30. Hunter DB, Smith HV (2005) A quadrature formula of Clenshaw–Curtis type for the Gegenbauer weight-function. J Comput Appl Math 177:389–400
31. Jerison DS, Kenig CE (1981) The Neumann problem on Lipschitz domains. Bull Am Math Soc (N.S.) 4:203–207
32. John F (1991) Partial differential equations, vol 1. Springer, New York
33. Kondrat′ev VA (1967) Boundary value problems for elliptic equations in domains with conical or angular points. Trans Moscow Math Soc 16:227–313
34. Kozlov VA, Maz′ya VG, Rossmann J (1997) Elliptic boundary value problems in domains with point singularities. Mathematical surveys and monographs, vol 52. American Mathematical Society, Providence
35. Kress R (1989) Linear integral equations, vol 82. Springer, Berlin
36. Kress R (1990) A Nyström method for boundary integral equations in domains with corners. Numer Math 58:145–161
37. Lin K, Tong P (1980) Singular finite elements for the fracture analysis of V-notched plate. Int J Numer Methods Eng 15:1343–1354

38. Maischak M, Stephan EP (1997) The *hp*-version of the boundary element method in $\mathbf{R}^3$: the basic approximation results. Math Methods Appl Sci 20:461–476
39. Maue A-W (1949) Zur Formulierung eines allgemeinen Beugungsproblems durch eine Integralgleichung. Z Phys 126:601–618
40. Monegato G, Scuderi L (2003) A polynomial collocation method for the numerical solution of weakly singular and nonsingular integral equations on non-smooth boundaries. Int J Numer Methods Eng 58:1985–2011
41. Rokhlin V (1993) Diagonal forms of translation operators for the Helmholtz equation in three dimensions. Appl Comput Harmon Anal 1:82–93
42. Sloan IH, Smith WE (1980) Product integration with the Clenshaw–Curtis points: implementation and error estimates. Numer Math 34:387–401
43. Song J, Lu C, Chew W, Lee S (1998) Fast Illinois Solver Code (FISC). IEEE Antennas Propag Mag 40:27–34
44. Stern M (1979) Families of consistent conforming elements with singular derivative fields. Int J Numer Methods Eng 14:409–421
45. Strain J (1995) Locally corrected multidimensional quadrature rules for singular functions. SIAM J Sci Comput 16:992–1017
46. Trefethen LN (2008) Is Gauss Quadrature Better than Clenshaw-Curtis? SIAM Rev 50:67–87
47. Weideman JAC, Trefethen LN (2007) The kink phenomenon in Fejér and Clenshaw-Curtis quadrature. Numer Math 107:707–727
48. Verchota G (1984) Layer potentials and regularity for the Dirichlet problem for Laplace's equation in Lipschitz domains. J Funct Anal 59:572–611
49. Wigley NM (1964) Asymptotic expansions at a corner of solutions of mixed boundary value problems. J Math Mech 13:549–576
50. Wigley NM (1969) On a method to subtract off a singularity at a corner for the Dirichlet or Neumann problem. Math Comput 23:395–401
51. Wigley NM (1987) Stress intensity factors and improved convergence estimates at a corner. SIAM J Numer Anal 24:350–354
52. Wu X, Xue W (2003) Discrete boundary conditions for elasticity problems with singularities. Comput Methods Appl Mech Eng 192:3777–3795
53. Wu X, Han H (1997) A finite-element method for Laplace- and Helmholtz-type boundary value problems with singularities. SIAM J Numer Anal 34:1037–1050
54. Zargaryan SS, Maz′ya VG (1984) The asymptotic form of the solutions of integral equations of potential theory in the neighbourhood of the corner points of a contour. Prikl Mat Mekh 48:169–174